

Semantic-Enhanced Time-Series Forecasting via Large Language Models

Hao Liu¹ Chun Yang¹, Xiaoxing Zhang², Xiaobin Zhu¹

¹University of Science and Technology Beijing

²Yizhi, China Telecom

d202410441@xs.ustb.edu.cn, chunyang@ustb.edu.cn, zhangxx7@chinatelecom.cn, zhuxiaobin@ustb.edu.cn,

Abstract

Time series forecasting plays a significant role in finance, energy, meteorology, and IoT applications. Recent studies have leveraged the generalization capabilities of large language models (LLMs) to adapt to time series forecasting, achieving promising performance. However, existing studies focus on token-level modal alignment, instead of bridging the intrinsic modality gap between linguistic knowledge structures and time series data patterns, greatly limiting the semantic representation. To address this issue, we propose a novel Semantic-Enhanced LLM (SE-LLM) that explores the inherent periodicity and anomalous characteristics of time series to embed into the semantic space to enhance the token embedding. This process enhances the interpretability of tokens for LLMs, thereby activating the potential of LLMs for temporal sequence analysis. Moreover, existing Transformer-based LLMs excel at capturing long-range dependencies but are weak at modeling short-term anomalies in time-series data. Hence, we propose a plugin module embedded within self-attention that models long-term and short-term dependencies to effectively adapt LLMs to time-series analysis. Our approach freezes the LLM and reduces the sequence dimensionality of tokens, greatly reducing computational consumption. Experiments demonstrate the superiority performance of our SE-LLM against the state-of-the-art (SOTA) methods.

Introduction

Time series forecasting has widespread applications in various tasks, such as finance, energy, meteorology, and industrial IoT (Liu et al. 2016; Arslan 2022; Sherstinsky 2018). Recently, Transformer-based LLMs (Radford et al. 2019; Devlin et al. 2019; Yang et al. 2024a; Touvron et al. 2023) are prevalent in time series forecasting (Jin et al. 2024; Liu et al. 2024c, 2025; Hu et al. 2025) by integrating multi-domain knowledge to model temporal dependencies, thereby enhancing time series analysis effectively.

Time series data fundamentally differs from linguistic structures in nature. Existing methods often convert temporal information into textual prompts to activate the potential of LLMs. GPT4mTS (Jia et al. 2024a) introduces a prompt-based framework that jointly processes temporal data and textual information. Zhou et al. (Zhou et al. 2023) processed time-series data by randomly initializing the embedding layer and directly performing serialized analysis through frozen LLMs. However, the inherent modality gap

between temporal and linguistic data resulted in low-quality embeddings. In this regard, LLM4TS (Chang et al. 2025) introduces a unified framework that fuses token, positional, and temporal embeddings to maintain modality consistency. Time-LLM (Jin et al. 2024) converts time-series data into text prototype representations and integrates textual prompts to enhance time series analysis. Meanwhile, S2IP-LLM (Pan et al. 2024a) incorporates time-series data into LLM’s semantic space as prompts, compensating for the lack of textual prompts. However, incorporating textual information may introduce noise (Liu et al. 2025), and the text descriptions incur additional computational cost (Lin et al. 2024; Ma et al. 2023; Shang et al. 2024).

Most existing LLM-based methods mainly focus on token-level alignment (Hu et al. 2025), as shown in Fig. 1 (a) (Pan et al. 2024a; Liu et al. 2025). The joint space serves as an implicit prompt, guiding the LLM in conducting time series forecasting. Semantic tokenization eliminates the dependency on auxiliary textual descriptions. However, this token-level alignment overlooks temporal and channel dependencies, making it difficult to capture dynamic temporal patterns. To address these limitations, our analysis identifies a critical oversight in existing LLM-based approaches (Jin et al. 2024; Liu et al. 2024c; Chang et al. 2025; Zhou et al. 2023). Regarding the semantic space composed of tokens and time steps, we propose the Temporal-Semantic Cross-Correlation (TSCC) Module to obtain enhanced semantics that represent temporal patterns, emphasize anomaly and de-anomaly patterns, thereby enhancing the interpretability of the token embeddings, as shown in Fig. 1 (b). Although we provide semantic guidance with high interpretability from LLMs, there exists an inherent difference between LLMs’ understanding of linguistic knowledge and temporal pattern. We propose to freeze the LLM and introduce an adapter to transform the model’s semantic information into the capability of modeling dynamic changes in time series, as shown in Fig. 1 (c).

In summary, we propose Semantic-Enhanced LLM, a novel framework that enhances LLM for time series forecasting with two key components: the Temporal-Semantic Cross-Correlation (TSCC) module and the Time-Adapter architecture. The TSCC captures cross-correlation of temporal embedding and semantic space with temporal dependencies and channel-wise relationships, which embed into token

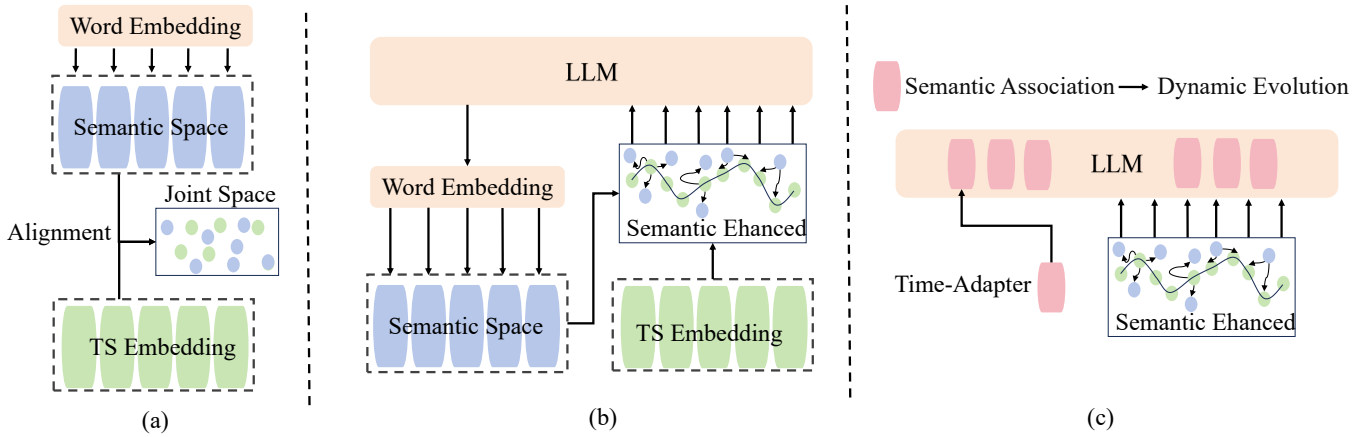


Figure 1: (a) The input time series is mapped to obtain time series (TS) Embeddings. Next, the feature space is aligned with the semantic space derived from the pre-trained word token embedding. (b) Temporal patterns are injected into the joint space and use implicit prompts to LLM for forecasting. (c) Embedding Time Adapter enhances learning of temporal patterns.

embedding to adapt LLM to temporal features. The Time-Adapter enhances forecasting capability by overcoming the limitation of LLMs in modeling both short-term and long-term dependencies based on historical time segments. This enables pretrained LLMs to forecast time series effectively. Our main contributions are four-fold:

- We introduce a novel SE-LLM to bridge the inherent modal differences between time series and language data, activating the generalization capability of LLMs for time-series analysis.
- We propose a novel Temporal-Semantic Cross-Correlation (TSCC) module to enhance token embedding by endowing semantic information with temporal patterns, which improves temporal analysis.
- We propose a Time-Adapter to bridge the modality gap between LLMs and time-series data, effectively modeling both long-term dependencies and short-term patterns.
- Extensive experiments verify the superior performance and efficiency of our SE-LLM.

Related Works

Time Series Forecasting

Traditional time series forecasting methods, such as ARIMA (Liu et al. 2016) and Prophet (Arslan 2022), often relied on statistical and classical machine learning techniques. The rise of deep learning brought Recurrent Neural Networks (RNNs) (Sherstinsky 2018; Qin et al. 2017; Yeo et al. 2018; Khaldi et al. 2023), which excelled at modeling temporal dependencies. Long Short-Term Memory (LSTM) networks (Kong et al. 2025; Shahzad et al. 2023) improved RNNs by addressing vanishing gradients and long-range dependencies. Advances PGN (Jia et al. 2024b) further enhanced long-term temporal relationship modeling, and improved computational efficiency. Concurrently, Graph Neural Networks (GNNs) (Cao et al. 2020; Pan et al. 2024b; Deng et al. 2020) excelled at capturing spatial and structural dependencies in spatiotemporal contexts. Recently,

Transformer-based architectures (Chen et al. 2021; Zhang and Yan 2023; Wang et al. 2024) have dominated due to their ability to capture global temporal patterns. However, these models struggle with generalizability and flexibility in highly dynamic, real-world time series analysis.

LLM-based Time Series Forecasting

Recently, LLMs (Radford et al. 2019; Touvron et al. 2023; Zhang et al. 2022; DeepSeek-AI 2024; Yang et al. 2024a) have developed rapidly, and demonstrated significant potential in advancing time-series forecasting. Gruver *et al.* (Gruver et al. 2023) and Xue *et al.* (Xue and Salim 2023) reformulated forecasting as a sentence-to-sentence translation task to bridge the modality gap. Time-LLM (Jin et al. 2024) leverages token-level embedding as a prompt to enhance the textual description to enhance LLM’s understanding of temporal concepts. Pan *et al.* (Pan et al. 2024a) integrate semantic space with embedding as a prompt to guide LLM. Liu *et al.* (Liu et al. 2025) indicate that the embedding of textual information is weak, and they proposed an entangled reliable embedding. Hu *et al.* (Hu et al. 2025) introduced FSCA, which utilizes Graph Neural Networks (GNNs) to ensure structural and logical alignment. Auto-Times (Liu et al. 2024c) explored autoregressive forecasting with timestamp embedding to improve LLM’s performance. Notably, the aforementioned studies and most research (Jia et al. 2024a) employ a frozen LLM approach for time series learning, indicating that LLMs have already acquired rich general semantic recognition capabilities during the pre-training weight. If all parameters are directly finetuned, these general capabilities may be compromised, leading to unstable performance in time series tasks. Current research merely leverages the generalization ability of LLMs for downstream tasks, suggesting that the inherent architecture of LLMs is not well-suited for time series forecasting.

Adapter-based LLM Fine-Tune

Existing methods show that fine-tuning LLMs (Jin et al. 2024; Zhou et al. 2023; Gruver et al. 2023) not only consumes computational resources but also degrades forecasting performance across data from different domains. Adapter-based fine-tuning techniques (Hu et al. 2022; Guo et al. 2024; Zhang et al. 2023; Zhang, Zhu, and Gao 2025; Lester, Al-Rfou, and Constant 2021) have demonstrated efficient adaptation to task-specific distributions in various tasks (Liu et al. 2024a; Chen, Jie, and Ma 2024; Mu et al. 2025). Empirical studies, e.g., Gupta *et al.* (Gupta et al. 2024), validate the effectiveness of LoRA-style fine-tuning in boosting time-series forecasting performance. AutoTimes (Liu et al. 2024c) incorporates LoRA (Hu et al. 2022) into GPT-2 (Radford et al. 2019), achieving substantial improvements in long-range prediction scenarios. However, the success of these fine-tuning techniques is highly contingent upon algorithmic design choices (Pan et al. 2024a; Zhou et al. 2023; Jin et al. 2024), and the transferability of these methods across diverse time-series domains remains unclear. We contend that current adapters, while enhancing LLMs’ understanding of semantic structures, are not designed to capture temporal patterns effectively. In contrast, the Time-Adapter is specifically designed to model short- and long-term dependencies, boosting LLMs adapt to temporal forecasting tasks.

Methods

The Overview of SE-LLM

The proposed SE-LLM model consists of two primary components: the TSCC and the Time-Adapter, as depicted in Fig. 2. The process begins with the input sequence, a time series data matrix with batch size \mathbf{B} and sequence length \mathbf{L} . A sliding window operation is applied to partition the temporal dimension into smaller segments, restructuring the representation and reducing computational complexity from $\mathcal{O}(L^2)$ to $\mathcal{O}(N^2K)$, where $\mathbf{T} \rightarrow \tilde{\mathbf{T}}$, $\tilde{\mathbf{T}} \in \mathbb{R}^{B \times N \times K}$. This design reduces self-attention and feed-forward network complexities, improving the model’s efficiency.

TS Embedding. The temporal representation is passed through the Time Encoder module, which projects the data into a high-dimensional TS Embeddings, which can be formulated as:

$$\mathbf{H} = \mathcal{F}_2 \left(\sigma \left(\mathcal{F}_1(\tilde{\mathbf{T}}) \right) \right), \quad (1)$$

where $\mathbf{H} \in \mathbb{R}^{B \times N \times C}$, $\mathcal{F}_1, \mathcal{F}_2$ is linear model, σ is activation. This projection captures more expressive features of the temporal patterns within the data.

Semantic Space. The semantic space is the semantic embedding obtained by mapping the word embedding of a large language model through a linear layer, which we collectively refer to as the semantic space. Specifically, we map the Word Embedding layer from $W \in \mathbb{R}^{V \times C}$ to $S \in \mathbb{R}^{K \times C}$ (Fang et al. 2025). The pre-trained word embeddings from LLM are used as general features, and a linear transformation is applied to transfer the features to a new semantic space, allowing the model to match the time series of the TS Embeddings.

We input both the semantic space and temporal features into the TSCC to obtain enhanced semantics, as shown in Fig. 2(b). Following this, the LLM embeds Time-Adapter into the Multi-Head Attention to further refine the model’s ability to understand temporal patterns in the time series data, as shown in Fig. 2(c). This component enhances the overall temporal pattern recognition by integrating additional contextual information, enabling better forecasting performance. Finally, the Decoder component decodes the output from the LLM to produce the final prediction as:

$$\mathbf{O} = \mathcal{F}_2 \left(\sigma \left(\mathcal{F}_1(\mathbf{Y}) \right) \right), \quad (2)$$

where \mathbf{Y} is the LLM’s output. The test processes are provided in Appendix A.

Temporal-Semantic Cross-Correlation

Fig. 3 is the architecture of the TSCC module. The core of this module is to infuse temporal patterns into the joint space. Firstly, we align the temporal embeddings with the semantic space through a cross-attention mechanism (Jin et al. 2024; Liu et al. 2025; Chang et al. 2025).

Cross-Modality Alignment. The Cross-Domain Attention Mechanism is capable of dynamically capturing complex associations between different modalities, and achieving efficient fusion through adaptive weight allocation. Hence, we employ Cross Attention to align temporal embeddings with the semantic space, thereby obtaining Joint Space (JS) $\mathbf{C} \in \mathbb{R}^{B \times N \times C}$. This can be formulated as:

$$\mathbf{C} = \text{CrossAttn}(S, H). \quad (3)$$

Anomaly Pattern Modeling. In time series analysis, the anomaly noise in non-stationarity information lead to inaccurate model parameter estimation and increased prediction bias. We employ a Anomaly Modeling Variational Autoencoder (AM-VAE) (Cemgil et al. 2020) to reconstruct the mean and variance in a joint space, comprehensively capturing the underlying stochastic process of anomaly noise in temporal data, as described in Algorithm 1. The reconstruction process eliminates the reconstruction loss function, enabling the model to allow the latent variable distribution to dynamically adapt over time, thereby capturing temporal pattern.

Temporal Pattern Infusion. The cross-correlation matrix \mathbf{M} is computed via standardization over both temporal and semantic features, which can be formulated as:

$$\mathbf{M} = \frac{\mathbf{H} - \mu_H}{\sigma_H} \times \frac{S^T - \mu_S}{\sigma_S}. \quad (4)$$

Followed by a top-K (Liu et al. 2024a) filtering mechanism to select the most strongly correlated positions and weighted to the output of AM-VAE to endow both anomaly and de-anomaly semantics with a temporal features that exhibits strong correlations. It can be formulated as:

$$\begin{aligned} \overline{\mathbf{DA}} &= \mathbf{DA} \cdot \frac{1}{n} \sum_{i=1}^n \mathcal{P}(S_i, m_{\text{top}_k}^i), \\ \overline{\mathbf{DC}} &= \mathbf{DC} \cdot \frac{1}{n} \sum_{i=1}^n \mathcal{P}(S_i, m_{\text{top}_k}^i), \end{aligned} \quad (5)$$

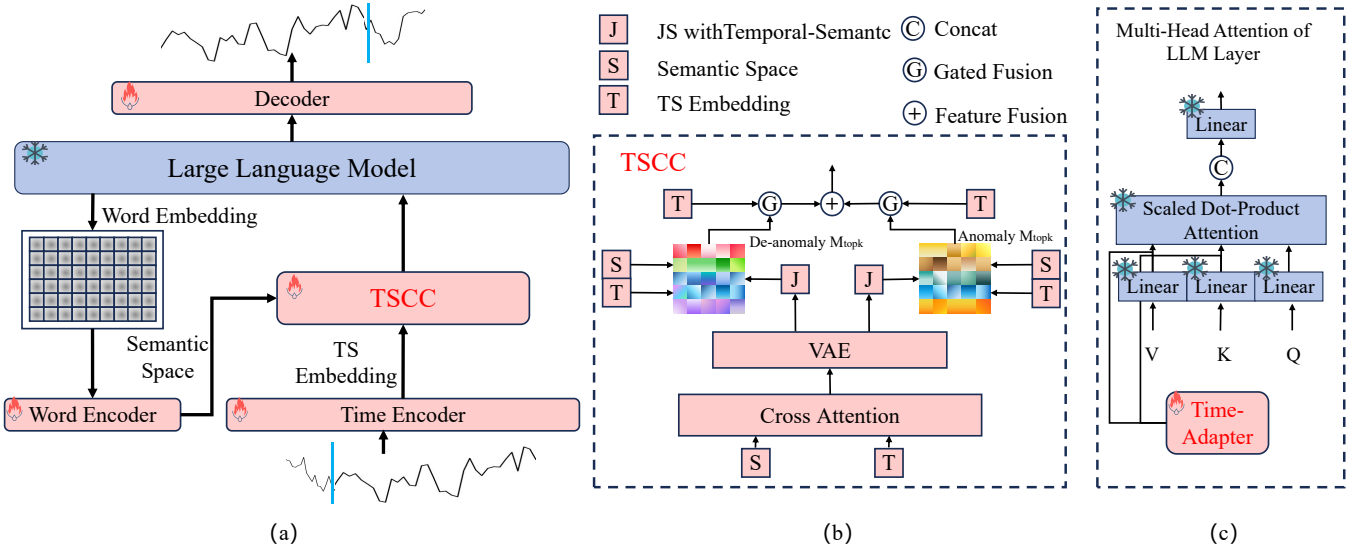


Figure 2: (a) An overview of SE-LLM. Red indicates trainable, while blue indicates frozen. (b) The overall framework of TSCC, with detailed processes referring to Fig. 3. (c) For the Transformer-based LLM, the Time-Adapter is embedded within the key and value vectors of the multi-head attention mechanism. JS is an abbreviation for Joint Space.

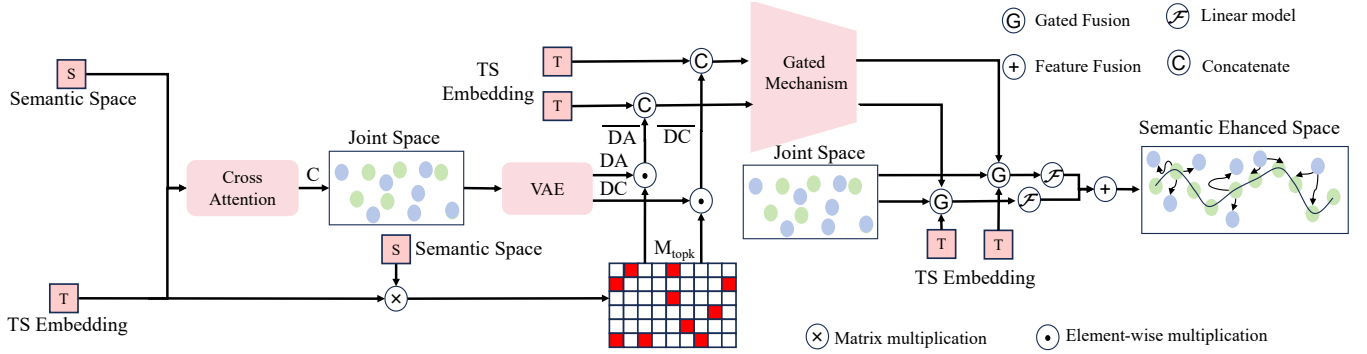


Figure 3: Architecture of TSCC module, where \overline{DA} and \overline{DC} correspond to "de-anomaly semantic" and "anomaly semantic".

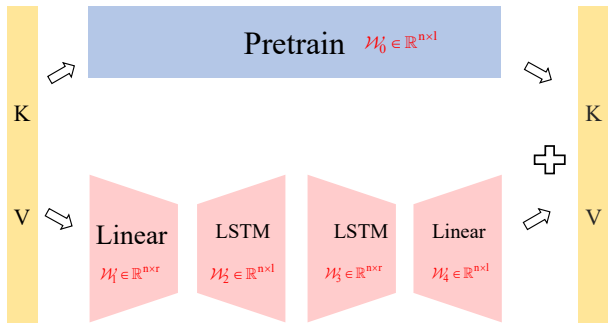


Figure 4: The architecture of Time-Adapter, a modular enhancement designed to improve the temporal modeling capabilities of LLMs. It comprises two linear layers and two parallel LSTM modules, enabling effective capture of both long-term and short-term temporal dependencies.

where \overline{DC} represents enhanced anomaly semantics reconstructed by the AM-VAE module from the joint space, \overline{DA} represents enhanced de-anomaly semantics, \mathcal{P} represents the matrix in the semantic space corresponding to the indices of the top-k positions in the cross-correlation matrix.

Channel Dependency Enhancement. The aforementioned enhanced semantics are learned by integrating the temporal features TS. To prevent the loss of feature information, we further acquire channel dependencies based on the enhanced semantics modeled along the temporal dimension. Specifically, we concatenate the TS Embeddings and the \overline{DA} , \overline{DC} , that share information across channel dimensions. We employ a Multi-Layer Perceptron (MLP) for attention extraction, perform channel enhancement on the enhanced semantics in channel dimension, which can be formulated as:

$$\text{Attn}_a = \text{MLP}([H, \overline{DA}]), \quad (6)$$

where \overline{DC} has same processed to get Attn_c , and we will mainly focus on introducing DA.

Algorithm 1: Anomaly Noise Modeling via AM-VAE Module

Require: Cross-attention output: Joint Space $\mathbf{C} \in \mathbb{R}^{B \times N \times C}$

Ensure: Decomposed anomaly semantic **DC** and de-anomalized semantic **DA** with temporal pattern

- 1: **Latent Feature Projection:** $\mathbf{V} \leftarrow \sigma(\mathcal{F}_e(\mathbf{C}))$, where \mathcal{F}_e : Linear mapping from $\mathbb{R}^C \rightarrow \mathbb{R}^n$
 - 2: **Latent Distribution Estimation:** $\mu, \log \sigma^2 \leftarrow \mathcal{F}_\mu(\mathbf{V}), \mathcal{F}_\sigma(\mathbf{V})$, where $\mathcal{F}_\mu, \mathcal{F}_\sigma$: Linear mapping from $\mathbb{R}^n \rightarrow \mathbb{R}^m$.
 - 3: **Reparameterization Trick:** Sample from latent space, $\mathbf{z} \leftarrow \mu + \epsilon \odot \exp(0.5 \cdot \log \sigma^2) \leftrightarrow z = \mu + \epsilon \odot \sigma$, $\epsilon \sim \mathcal{N}(0, \mathbf{I})$.
 - 4: **Anomaly Sample:** In time series forecasting, the true observations are modeled as: $\mathbf{b}_t = f(a_t) + \eta$, where $f(a_t)$ is a prediction function based on historical data, and η is a random noise term. We assume that future values follow a certain distribution, for example: $\mathbf{b}_t \sim (\mu_t, \sigma_t^2)$. The prediction not a single point estimate, but a probability distribution. To generate possible future trajectories, sampling from this distribution is required: $\mathbf{b}_t = \mu_t + \epsilon \cdot \sigma_t$, where $\epsilon \sim N(0, 1)$. The statistical characteristics of the noise may vary over time, which corresponds precisely to the per-timestep application of the **Reparameterization Trick**.
 - 5: **Anomaly Semantic Modeling:** Decode latent variable to recover anomaly semantic, $\mathbf{DC} \leftarrow \mathcal{F}_d(\mathbf{z})$, $\mathcal{F}_d : \mathbb{R}^m \rightarrow \mathbb{R}^C$
 - 6: **Anomaly Decomposition:** $\mathbf{DA} = \mathbf{C} - \mathbf{DC}$, $\mathbf{DC} \in \mathbb{R}^{B \times N \times C}$, $\mathbf{DA} \in \mathbb{R}^{B \times N \times C}$, where **DC** represents the latent anomaly noise semantic in joint space, while **DA** represents the joint space where anomalous semantic are removed.
-

The **Attn** incorporates region weights that model the TS Embeddings from both channel and sequence dimensions, making it sensitive to temporal patterns. We employ a gating mechanism to integrate the semantic space and the TS Embeddings, thereby endowing the joint space with temporal patterns, it can be formulated as:

$$\mathbf{GA} = \mathcal{F}_{llm}(\text{Attn}_a \odot \mathbf{H} + (1 - \text{Attn}_a) \odot \mathbf{C}), \quad (7)$$

where, \mathcal{F}_{llm} is a linear layer that maps the enhanced semantics to the token space of the LLM. The resulting embeddings are enriched with semantic information that reflects temporal patterns. Finally, the de-anomalization ($\mathbf{GA} \in \mathbb{R}^{B \times N \times C}$) and anomaly ($\mathbf{GC} \in \mathbb{R}^{B \times N \times C}$) representations are mapped through a linear layer for alignment and fused to generate a unified semantic representation, which is more interpretable and suitable for LLMs analysis. It can be formulated as:

$$\mathbf{Y} = \text{LLM}(\mathbf{GA} + \mathbf{GC}). \quad (8)$$

This represents the fusion of the enhanced de-anomalized (**GA**) and anomalous (**GC**) semantics enriched with temporal patterns. The resulting unified representation is then processed through the LLM to analyze these enhanced semantics and generate a more accurate prediction.

Time-Adapter

Time-Adapter explicitly captures long-term and short-term dependencies, compensating for the Transformer’s inherent weaknesses in temporal pattern extraction, as shown in Fig. 4. Specifically, building upon LoRA (Hu et al. 2022), we replace the low-rank matrix with dual linear layers and introduce two parallel paths incorporating LSTM (Hochreiter and Schmidhuber 1997) units. These paths process temporal dependencies by leveraging long-range information from the Transformer’s architecture through nonlinear transformations, thereby equipping the model with temporal data-handling capabilities during training. The Time-Adapter module explicitly captures long-term and short-term dependencies by processing the temporal patterns through parallel LSTM paths. These dependencies are integrated into the key and value matrices of the multi-head attention mechanism. This enhancement enables the model to handle complex temporal patterns more effectively.

Our method consists of three key operations executed sequentially. First, a **Low-rank Projection** is applied, where a linear layer learns a low-rank matrix to reduce the input dimensionality. Then the **Long-term Dependency Modeling**, in which an LSTM (Zhang et al. 2022) maps the compressed features to a high-dimensional space, effectively capturing long-term temporal patterns. Finally, **Short-term Dependency Modeling** is performed, where a second LSTM processes the high-dimensional representation via a reverse projection (high-to-low mapping), isolating localized short-term dynamics. Finally, a linear layer integrates these refined temporal dependencies into the key ($\mathbf{k} \in \mathbb{R}^{B \times N \times C}$) and value ($\mathbf{v} \in \mathbb{R}^{B \times N \times C}$) matrices of the self-attention mechanism, enhancing their capacity to model temporal relationships.

Experiments

The evaluation metrics, datasets, and baseline methods are provided in the Appendix B.1.

Comparative Results

Long-Term Forecasting. Long-term forecasting faces challenges such as trend drift, structural changes, periodic fluctuations, and noise accumulation. These difficulties make it an important yet demanding task in time-series forecasting. The long-term forecasting results are provided in Table 1. SE-LLM achieves superior accuracy on ETTh1, Traffic, ECL, and Solar. On the Traffic dataset, which contains highly nonlinear patterns with strong variability, our approach obtains a 4.4% reduction in MSE compared with the best baseline. On ECL, SE-LLM also reaches the best performance and shows strong stability under periodic consumption patterns. For ETTh1 and Solar, where seasonal and trend components are pronounced, our method maintains competitive accuracy across all horizons. Some results are missing because several previous methods do not provide accessible code or cannot be applied to specific datasets due to design constraints. All reported comparisons follow identical training and evaluation settings. Overall, the results indicate that SE-LLM reduces long-horizon degradation and preserves high accuracy

Table 1: The input length of the SE-LLM is 672. The forecast horizon is {96, 192, 336, 720}. The best results are in **red** and the second best are **blue**. Full results are provided in Table 9.

Models	SE-LLM		TimXier++ 2025		TimeMOE 2025		Time-CMA 2025		TQNet 2025		LLM-TS 2025		AutoTimes-GPT2 2024		Time-LLM 2024		iTransFormer 2024		
	MSE	MAE	MSE	MAE	MSE	MAE	MSE	MAE	MSE	MAE	MSE	MAE	MSE	MAE	MSE	MAE	MSE	MAE	
Merits																			
ETTh1	0.381	0.415	0.429	0.443	0.412	0.426	0.396	0.419	0.438	0.450	0.454	0.451	0.397	0.425	0.448	0.443	0.421	0.445	
Weather	0.229	0.267	0.228	0.226	0.288	0.344	0.25	0.476	0.227	0.268	0.257	0.285	0.242	0.281	0.227	0.266	0.266	0.291	
Traffic	0.386	0.261	0.404	0.311	—	—	—	—	0.400	0.278	0.618	0.333	0.406	0.276	0.402	0.294	0.384	0.274	
ECL	0.161	0.255	0.163	0.257	0.256	0.289	0.185	0.287	0.161	0.259	0.173	0.266	0.173	0.268	0.207	0.306	0.164	0.258	
Solar	0.192	0.242	0.194	0.256	—	—	0.227	0.276	0.230	0.270	—	—	0.207	0.246	0.234	0.293	0.213	0.291	

Table 2: The M4 dataset includes yearly, quarterly, monthly, weekly, daily, and hourly data, the short-term forecasts averaged across all M4 subsets. Full results are provided in Table 10.

Models		SE-LLM	TimeMixer++ 2025	FSCA 2025	Time-VLM 2025	AutoTimes 2024	S2IP-LLM 2024	Time-LLM 2024	FPT 2024	iTransformer 2024
		Average	SMAPE	11.778	11.884	11.828	11.894	11.831	12.021	11.983
	MASE	1.578	1.597	1.580	1.592	1.585	1.612	1.595	1.600	1.631
	OWA	0.847	0.856	0.850	0.855	0.850	0.857	0.859	0.861	0.874

across diverse data distributions, confirming its effectiveness in long-term forecasting.

Short-Term Forecasting. It refers to predicting target variables within a relatively brief future time horizon. We have meticulously selected algorithms suitable for short-term forecasting for comparison. SE-LLM was compared with the SOTA models in short-term forecasting on the M4 dataset, as shown in Table 2, and the results demonstrated that we achieved the best performance. Our method achieved a 0.26% reduction in Symmetric Mean Absolute Percentage Error (SMAPE), a 0.94% decline in Mean Absolute Scaled Error (MASE), and a 0.47% decrease in Quantile-Weighted Absolute Error (QWA) relative to the second best. This indicates that SE-LLM has the ability to capture short-term time-varying patterns through enhanced short-term dependencies.

Zero-Shot forecasting. The TSCC module utilizes the AM-VAE to construct simulated anomaly data, facilitating the learning of latent distribution characteristics in time series data. This enables the model to better generalize to unseen temporal patterns, making it well-suited for zero-shot forecasting. The ability to generalize across different datasets is critical for this task, as the model must adapt to varying data distributions and temporal structures without prior training on those specific patterns. We conducted zero-shot prediction experiments on the univariate M3 and M4 datasets, which exhibit various temporal variation patterns and different data distributions. Unlike many existing methods that struggle with such generalization, our model leverages the latent space learned by AM-VAE to capture underlying temporal structures that facilitate transferability across domains. Specifically, the M3 and M4 datasets present distinct temporal patterns (e.g., from quarterly to monthly or daily frequencies), and our approach benefits from the generalization capability afforded by the AM-VAE to simulate realistic temporal patterns, even in the absence of direct training data for those patterns.

In the zero-shot experiments, we compared our approach (SE-LLM) with several state-of-the-art methods (see Table 3) and found that SE-LLM outperformed others in zero-shot generalization. Notably, when transferring from M3 to M4, the SMAPE was reduced by 0.1% compared to AutoTimes, and by 1.4% when transferring from M4 to M3. These results underscore the model’s robustness in handling unseen data and diverse temporal patterns. Additionally, we examine domain generalization between the M3 and M4 datasets, where the temporal frequencies shift from monthly to weekly, daily, or hourly in the M3 → M4 transfer, and from quarterly to other frequencies in the M4 → M3 transfer. This domain adaptation capability, driven by the model’s ability to learn a shared latent structure across datasets, plays a key role in improving performance in zero-shot scenarios. The results further verify the model’s ability to generalize beyond the patterns seen during training.

Ablation Study

Ablation on Long-Term Forecasting. Ablation experiments are conducted on the ECL and Traffic datasets. To reduce computational costs, we selected different lightweight LLMs for comparison, including GPT2 (Radford et al. 2019), BERT (Devlin et al. 2019), Opt-125m (Zhang et al. 2022), and Qwen2.5-0.5B (Yang et al. 2024a), which are commonly used in current research (Zhou et al. 2023; Liu et al. 2024c, 2025; Jin et al. 2024). The experimental results are shown in Table 4. Our baseline uses a cross-domain attention mechanism for multi-modal alignment (Chang et al. 2025; Jin et al. 2024; Liu et al. 2025). After replacing it with the TSCC framework and adding the Time-Adapter, the prediction accuracy of different LLMs has improved, demonstrating the effectiveness of the innovative methods in this paper. Comparative experiments show Qwen-0.5B yields lower prediction errors among LLMs. The ablation study on short-term forecasting are provided in the Appendix B.3 and Table 13.

Table 3: The experimental results are based on the generalization of consistent temporal patterns. For non-matching patterns, we evaluate frequency transfers from Monthly to Weekly/Daily/Hourly in the M3 → M4 dataset, and from Quarterly to other frequencies in the M4 → M3 dataset. Full result are shown in Table 11.

Method	SE-LLM	AutoTimes	FPT	Dlinear	PatchTST	TimesNet	FEDformer	Informer	Reformer
M3→M4	13.024	13.036	13.125	15.337	13.228	14.553	15.047	19.047	14.092
M4→M3	12.560	12.750	13.060	14.030	13.390	14.170	13.530	15.820	13.370

Table 4: In the ablation experiments, we set the input length to 672 and the output length to 96, with forecast lengths from the set {96, 192, 336, 720}. Full results are provided in Table 12.

LLM	GPT2				Bert				Opt125m				Qwen2.5-0.5B			
	ECL		Traffic		ECL		Traffic		ECL		Traffic		ECL		Traffic	
Mertic	MSE	MAE														
Baseline	0.179	0.270	0.422	0.284	0.184	0.276	0.472	0.321	0.173	0.267	0.403	0.280	0.167	0.263	0.405	0.279
+TSCC	0.172	0.264	0.409	0.280	0.177	0.270	0.431	0.294	0.170	0.263	0.396	0.270	0.166	0.262	0.389	0.264
+Time-Adapter	0.166	0.258	0.406	0.279	0.167	0.260	0.412	0.282	0.163	0.257	0.391	0.266	0.161	0.255	0.386	0.261

Table 5: Ablation study results on the ETTh1 dataset, where checkmarks indicate the modules employed, showing the results for different prediction horizons. All the strategies together yield the best results marked in red.

Module Ablation				96		192		336		720		Avg	
AM-VAE	Cross_Attn	Gated_Fusion	Semantic Space	MSE	MAE								
✓	✓	✓	✓	0.355	0.396	0.390	0.418	0.408	0.431	0.419	0.448	0.393	0.423
✓	✓	✓	✓	0.358	0.397	0.392	0.419	0.410	0.432	0.423	0.450	0.396	0.425
✓	✓	✓	✓	0.366	0.405	0.398	0.427	0.412	0.438	0.421	0.456	0.399	0.432
✓	✓	✓	✓	0.364	0.401	0.397	0.426	0.414	0.439	0.433	0.458	0.402	0.431
✓	✓	✓	✓	0.352	0.393	0.378	0.411	0.391	0.420	0.402	0.437	0.381	0.415

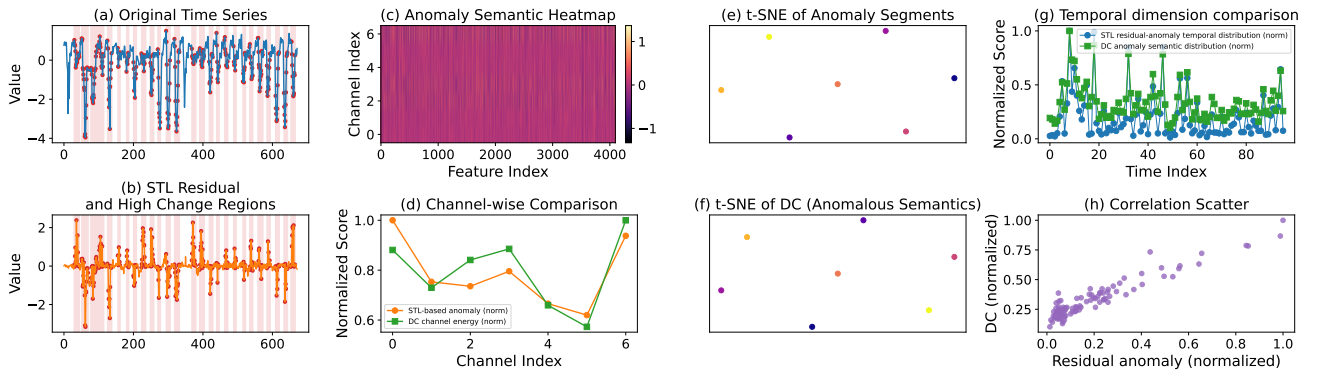


Figure 5: Qualitative analysis illustrating how the AM-VAE effectively models anomaly patterns.

Ablation on TSCC Module. The TSCC module features a sophisticated architecture. To better understand the contribution of each component, we perform a systematic ablation study, as summarized in Table 5. Specifically, we investigate the impact of removing or modifying key elements: (1) The AM-VAE module is removed to assess how the absence of simulated noisy data affects the modeling of temporal patterns. (2) The cross-domain attention mechanism is replaced with a simple linear layer for feature concatenation, thereby altering the approach to dynamic alignment and fusion across domains. (3) The gated attention mechanism is eliminated to examine the importance of capturing channel-

wise dependencies. (4) Finally, the semantic space is substituted with a learnable parameter matrix, aiming to implicitly approximate the large language model’s embedding without explicit semantic guidance. Experimental results show that the TSCC module provides reliable input to the large language model by effectively mining temporal patterns, injecting them into the semantic space, and employing an implicit prompting strategy.

Qualitative Analysis on TSCC Module. In Fig. 5, (a) we extract a segment from the ETTh dataset and apply STL decomposition to obtain the trend, seasonal, and residual components. The local deviations and abrupt fluctuations

Table 6: All reported results are averaged. Full results are provided in Tabel 14.

Datasets	ETTh1		Weather		Traffic		ECL		Solar	
Metrics	MSE	MAE								
Baseline-TSCC	0.381	0.415	0.242	0.287	0.389	0.264	0.166	0.262	0.201	0.251
+LoRA	0.396	0.425	0.240	0.278	0.390	0.268	0.163	0.257	0.202	0.253
+Time-Adapter	0.389	0.420	0.229	0.267	0.386	0.261	0.161	0.255	0.192	0.243

Table 7: The forecasting horizons are in $\{96, 192, 336, 720\}$, and all experimental results presented are averages. Full results are provided in Table 15.

	Time-LLM		+TSCC		+Time-Adapter		AutoTimes		+TSCC		+Time-Adapter		Time-CMA		+TSCC	
	MSE	MAE	MSE	MAE	MSE	MAE	MSE	MAE	MSE	MAE	MSE	MAE	MSE	MAE	MSE	MAE
ETTh1	0.420	0.439	0.407	0.429	0.405	0.428	0.397	0.425	0.390	0.421	0.388	0.420	0.446	0.446	0.437	0.434
ETTh2	0.370	0.404	0.368	0.401	0.364	0.399	0.367	0.410	0.363	0.406	0.357	0.407	0.416	0.429	0.379	0.403
ETTh1	0.358	0.388	0.360	0.390	0.357	0.389	0.361	0.389	0.354	0.384	0.351	0.382	0.399	0.413	0.383	0.396
ETTh2	0.262	0.324	0.267	0.328	0.266	0.326	0.274	0.329	0.269	0.325	0.268	0.323	0.294	0.337	0.285	0.347

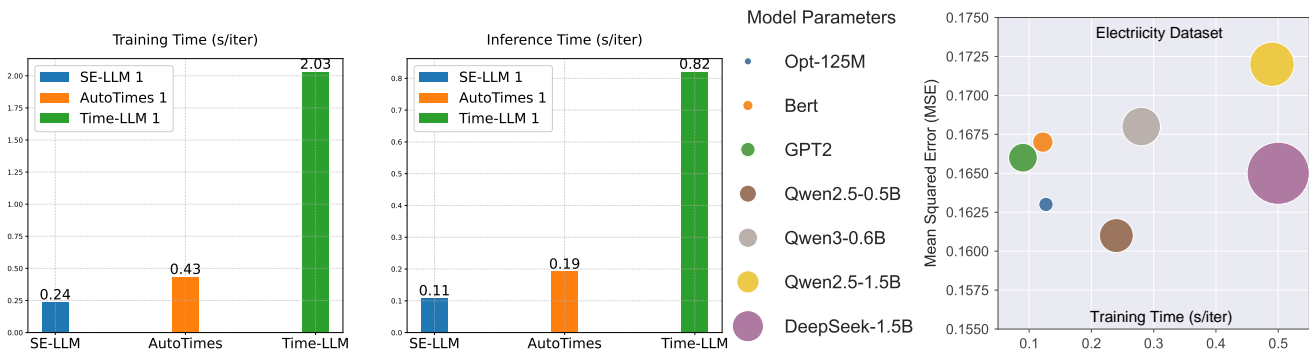


Figure 6: The size of the circles reflects the proportional relationship among the parameter counts of different LLMs.

in the residual component represent the anomalies that our AM-VAE is designed to capture. **(b)** STL decomposition reveals residual anomalies that are difficult to detect using traditional methods. The abrupt changes (marked by the red bar) are anomalous and challenging to explain, but our AM-VAE module effectively approximates these segments. The anomaly information is then analyzed using LLM’s generalization ability to uncover latent patterns in the semantic space. **(c)** The heatmap distribution of the noise semantics is shown. **(d)** demonstrates significant overlap between some channels and the anomalous segments in the residuals, indicating effective channel relationship mining for anomaly patterns. In **(e-f)**, the t-SNE analysis shows that the actual anomaly distribution and noise semantics form similar clusters. Seven tightly clustered points in the t-SNE projection reflect the alignment between the noise semantics and the identified anomalies, suggesting that the noise semantics closely resemble real anomalies, thus revealing latent patterns in the time series. In **(g)**, we show how noise semantics are regularized along the time dimension and compared with anomaly patterns. **(h)** The linear distribution in the correlation map confirms the close relationship between the two, indicating that the model captures the statistical properties of the anomaly patterns.

Ablation on Adapters. Long-term forecasting should

capture long-term dependencies, making the task more challenging. Therefore, to demonstrate the performance of Time-Adapter, we conducted a comparison with the LoRA (Hu et al. 2022; Liu et al. 2024c), and the results are presented in Table 6. The experimental baseline is the Qwen2.5 with the TSCC module. Experiments findings clearly demonstrate that LoRA lacks generalization capability to enhance forecasting performance. In contrast, Time-Adapter endows LLM with the ability to adapt to forecasting tasks.

Ablation on LLM-based SOTA methods. The modality gap between time-series and language data remains a challenging issue. To address this, we integrate TSCC and Time-Adapter as a plug-in into Time-LLM (Jin et al. 2024), AutoTimes (Liu et al. 2024c), and TimeCMA (Liu et al. 2025), evaluating their impact on the ETTh and ETTm datasets using the original code’s default parameters. All other settings remain unchanged, with GPT-2 consistently serving as the LLM backbone. Results in Table 7 show consistent error reductions, with TimeCMA achieving a notable drop in MSE. Since TimeCMA uses LLMs only to generate outputs from textual time-series prompts without training the LLM, ablation studies on Time-Adapter are not feasible. These results demonstrate that our approach addresses a common limitation across existing frameworks.

Efficiency Analysis

We evaluate the computational efficiency of our approach. All experiments were conducted with a batch size of 256 and a sequence length of 672, under which the training and inference times for each method were recorded. The bar chart in Fig. 6 compares the training and inference speeds of SE-LLM with classical algorithms, all evaluated on the same dataset, highlighting the superior efficiency of our method. In addition, the bubble chart illustrates the relationship between training speed and MSE variations on the ECL dataset when our approach is applied with different LLMs, further demonstrating the trade-offs between computational speed and prediction accuracy.

Conclusion

This paper introduces SE-LLM, which addresses the inherent modality gap between LLMs and time series data. We explore the temporal and channel dependencies between temporal embeddings and the semantic space of LLMs. Token embeddings are enhanced with temporal-pattern semantic information, improving interpretability and unlocking LLMs' potential. Moreover, we incorporate a plugin module tailored for time-series forecasting into LLMs, which activates their ability to model temporal dependencies. Experimental results demonstrate that SE-LLM surpasses SOTA performance. Furthermore, embedding TSCC and Time-Adapter into existing frameworks also leads to performance improvements, shedding light on common challenges in leveraging LLMs for time-series forecasting. SE-LLM efficiently integrates temporal information and language models.

Acknowledgements

This research is supported by National Science and Technology Major Project (2022ZD0119202), National Science Fund for Distinguished Young Scholars (62125601), National Natural Science Foundation of China (62576031).

Ethics Statement

This work focuses on advancing the methodology of time series forecasting by enhancing large language models (LLMs) with semantic structures derived from temporal data patterns. Our approach does not involve human subjects, personal data, or sensitive information, and all experiments are conducted on publicly available time series datasets. The proposed SE-LLM framework is designed to improve model interpretability and computational efficiency without altering the core parameters of the pre-trained LLM. We do not foresee direct societal harms from this research.

Reproducibility Statement

Our code is available, and the specific parameter configurations are provided within the code. All datasets used in the experiments are publicly available, and all compared baseline algorithms are from open-source projects. Our experimental results are reproducible.

This paper did not conduct ablation experiments using larger language models (e.g., Llama-7B or above) primarily because such large models incur significantly higher resource consumption compared to traditional time series forecasting methods, which goes against the requirement for lightweight applications. Although we propose a large language model-based algorithm for time series forecasting, we opted for a smaller-scale model to balance efficiency and practicality. Furthermore, we have already performed ablation analysis on large-parameter language models in the sections on Table 13 and Efficiency Analysis 4.3.

The discussion section of this paper is in Appendix C, and the limitations section is in Appendix D.

The usage of large language models is discussed in Appendix E.

References

- Arslan, S. 2022. A hybrid forecasting model using LSTM and Prophet for energy consumption with decomposition of time series data. *PeerJ Computer Science*, 8: 1001.
- Cao, D.; Wang, Y.; Duan, J.; Zhang, C.; Zhu, X.; Huang, C.; Tong, Y.; Xu, B.; Bai, J.; Tong, J.; and Zhang, Q. 2020. Spectral Temporal Graph Neural Network for Multivariate Time-series Forecasting. In *Advances in Neural Information Processing Systems*.
- Cemgil, A. T.; Ghaisas, S.; Dvijotham, K.; Gowal, S.; and Kohli, P. 2020. The Autoencoding Variational Autoencoder. In *Advances in Neural Information Processing Systems*.
- Chang, C.; Wang, W.; Peng, W.; and Chen, T. 2025. LLM4TS: Aligning Pre-Trained LLMs as Data-Efficient Time-Series Forecasters. *ACM Trans. Intell. Syst. Technol.*, 16(3): 60:1–60:20.
- Chen, C.; Oliveira, G. L.; Sharifi-Noghabi, H.; and Sylvain, T. 2025. LLM-TS Integrator: Integrating LLM for Enhanced Time Series Modeling. *Trans. Mach. Learn. Res.*, 2025.
- Chen, M.; Peng, H.; Fu, J.; and Ling, H. 2021. AutoFormer: Searching Transformers for Visual Recognition. In *International Conference on Computer Vision*, 12250–12260.
- Chen, S.; Jie, Z.; and Ma, L. 2024. LLaVA-MoLE: Sparse Mixture of LoRA Experts for Mitigating Data Conflicts in Instruction Finetuning MLLMs. *CoRR*, abs/2401.16160.
- DeepSeek-AI. 2024. DeepSeek-V2: A Strong, Economical, and Efficient Mixture-of-Experts Language Model. *CoRR*, abs/2405.04434.
- Deng, S.; Wang, S.; Rangwala, H.; Wang, L.; and Ning, Y. 2020. Cola-GNN: Cross-location Attention based Graph Neural Networks for Long-term ILI Prediction. In *International Conference on Information and Knowledge Management*, 245–254.
- Devlin, J.; Chang, M.; Lee, K.; and Toutanova, K. 2019. BERT: Pre-training of Deep Bidirectional Transformers for Language Understanding. In *North American Chapter of the Association for Computational Linguistics: Human Language Technologies*, 4171–4186.
- Fang, Z.; Zhu, X.; Yang, C.; Zhou, H.; Qin, J.; and Yin, X.-C. 2025. Aligning enhanced feature representation for

- generalized zero-shot learning. *Science China Information Sciences*, 68(2): 122102.
- Gruver, N.; Finzi, M.; Qiu, S.; and Wilson, A. G. 2023. Large Language Models Are Zero-Shot Time Series Forecasters. In *Advances in Neural Information Processing Systems*.
- Guo, H.; Greengard, P.; Xing, E. P.; and Kim, Y. 2024. LQ-LoRA: Low-rank plus Quantized Matrix Decomposition for Efficient Language Model Finetuning. In *International Conference on Learning Representations*.
- Gupta, D.; Bhatti, A.; Parmar, S.; Dan, C.; Liu, Y.; Shen, B.; and Lee, S. 2024. Low-Rank Adaptation of Time Series Foundational Models for Out-of-Domain Modality Forecasting. In *International Conference on Multimodal Interaction*, 382–386.
- Hochreiter, S.; and Schmidhuber, J. 1997. Long short-term memory. *Neural computation*, 9: 1735–1780.
- Hu, E. J.; Shen, Y.; Wallis, P.; Allen-Zhu, Z.; Li, Y.; Wang, S.; Wang, L.; and Chen, W. 2022. LoRA: Low-Rank Adaptation of Large Language Models. In *International Conference on Learning Representations*.
- Hu, Y.; Li, Q.; Zhang, D.; Yan, J.; and Chen, Y. 2025. Context-Alignment: Activating and Enhancing LLMs Capabilities in Time Series. In *International Conference on Learning Representations*.
- Jia, F.; Wang, K.; Zheng, Y.; Cao, D.; and Liu, Y. 2024a. GPT4MTS: Prompt-based Large Language Model for Multimodal Time-series Forecasting. In *AAAI Conference on Artificial Intelligence*, 23343–23351.
- Jia, Y.; Lin, Y.; Yu, J.; Wang, S.; Liu, T.; and Wan, H. 2024b. PGN: The RNN’s New Successor is Effective for Long-Range Time Series Forecasting. In *Advances in Neural Information Processing Systems*.
- Jin, M.; Wang, S.; Ma, L.; Chu, Z.; Zhang, J. Y.; Shi, X.; Chen, P.; Liang, Y.; Li, Y.; Pan, S.; and Wen, Q. 2024. Time-LLM: Time Series Forecasting by Reprogramming Large Language Models. In *International Conference on Learning Representations*.
- Khalidi, R.; Afia, A. E.; Chiheb, R.; and Tabik, S. 2023. What is the best RNN-cell structure to forecast each time series behavior? *Expert Systems with Applications*, 215: 119140.
- Kitaev, N.; Kaiser, L.; and Levskaya, A. 2020. Reformer: The Efficient Transformer. In *International Conference on Learning Representations*.
- Kong, Y.; Wang, Z.; Nie, Y.; Zhou, T.; Zohren, S.; Liang, Y.; Sun, P.; and Wen, Q. 2025. Unlocking the Power of LSTM for Long Term Time Series Forecasting. In *Association for the Advancement of Artificial Intelligence*, 11968–11976.
- Lai, G.; Chang, W.; Yang, Y.; and Liu, H. 2018. Modeling Long- and Short-Term Temporal Patterns with Deep Neural Networks. In *SIGIR Conference on Research & Development in Information Retrieval*, 95–104.
- Lester, B.; Al-Rfou, R.; and Constant, N. 2021. The Power of Scale for Parameter-Efficient Prompt Tuning. In *Empirical Methods in Natural Language Processing*, 3045–3059.
- Lin, S.; Chen, H.; Wu, H.; Qiu, C.; and Lin, W. 2025. Temporal Query Network for Efficient Multivariate Time Series Forecasting. In *International Conference on Machine Learning*, volume 267.
- Lin, S.; Lin, W.; Hu, X.; Wu, W.; Mo, R.; and Zhong, H. 2024. CycleNet: Enhancing Time Series Forecasting through Modeling Periodic Patterns. In *Advances in Neural Information Processing Systems*.
- Liu, C.; Hoi, S. C. H.; Zhao, P.; and Sun, J. 2016. Online ARIMA Algorithms for Time Series Prediction. In *AAAI Conference on Artificial Intelligence*, 1867–1873.
- Liu, C.; Xu, Q.; Miao, H.; Yang, S.; Zhang, L.; Long, C.; Li, Z.; and Zhao, R. 2025. TimeCMA: Towards LLM-Empowered Multivariate Time Series Forecasting via Cross-Modality Alignment. In *Association for the Advancement of Artificial Intelligence*, 18780–18788.
- Liu, S.; Zeng, Z.; Ren, T.; Li, F.; Zhang, H.; Yang, J.; Jiang, Q.; Li, C.; Yang, J.; Su, H.; Zhu, J.; and Zhang, L. 2024a. Grounding DINO: Marrying DINO with Grounded Pre-training for Open-Set Object Detection. In *European Conference on Computer Vision*, volume 15105, 38–55.
- Liu, Y.; Hu, T.; Zhang, H.; Wu, H.; Wang, S.; Ma, L.; and Long, M. 2024b. iTransformer: Inverted Transformers Are Effective for Time Series Forecasting. In *International Conference on Learning Representations*.
- Liu, Y.; Li, C.; Wang, J.; and Long, M. 2023. Koopa: Learning Non-stationary Time Series Dynamics with Koopman Predictors. In *Advances in Neural Information Processing Systems*.
- Liu, Y.; Qin, G.; Huang, X.; Wang, J.; and Long, M. 2024c. AutoTimes: Autoregressive Time Series Forecasters via Large Language Models. In *Advances in Neural Information Processing Systems*.
- Ma, S.; Zhang, T.; Zhao, Y.-B.; Kang, Y.; and Bai, P. 2023. TCLN: A Transformer-based Conv-LSTM network for multivariate time series forecasting. *Applied Intelligence*, 53(23): 28401–28417.
- Makridakis, S.; Spiliotis, E.; and Assimakopoulos, V. 2020. The M4 Competition: 100,000 time series and 61 forecasting methods. *International Journal of Forecasting*, 36(1): 54–74.
- Mu, J.; Wang, W.; Liu, W.; Yan, T.; and Wang, G. 2025. Multimodal Large Language Model with LoRA Fine-Tuning for Multimodal Sentiment Analysis. *ACM Trans. Intell. Syst. Technol.*, 16(6): 139:1–139:23.
- Nie, Y.; Nguyen, N. H.; Sinthong, P.; and *et al.* 2023. A Time Series is Worth 64 Words: Long-term Forecasting with Transformers. In *International Conference on Learning Representations*.
- Pan, Z.; Jiang, Y.; Garg, S.; Schneider, A.; Nevmyvaka, Y.; and Song, D. 2024a. S2IP-LLM: Semantic Space Informed Prompt Learning with LLM for Time Series Forecasting. In *International Conference on Machine Learning*.
- Pan, Z.; Jiang, Y.; Song, D.; Garg, S.; Rasul, K.; Schneider, A.; and Nevmyvaka, Y. 2024b. Structural Knowledge Informed Continual Multivariate Time Series Forecasting. *CoRR*, abs/2402.12722.

- Qin, Y.; Song, D.; Chen, H.; Cheng, W.; Jiang, G.; and Cottrell, G. W. 2017. In *International Joint Conference on Artificial Intelligence*, 2627–2633.
- Radford, A.; Wu, J.; Child, R.; Luan, D.; Amodei, D.; Sutskever, I.; et al. 2019. Language models are unsupervised multitask learners. *OpenAI blog*, 1(8): 9.
- Shahzad, Z.; Nadeem, A.; Saddam, H.; Algarni, A. D.; and Jawaid, I. 2023. A Multi Parameter Forecasting for Stock Time Series Data Using LSTM and Deep Learning Model. *Mathematics*, 11(3).
- Shang, Z.; Chen, L.; Wu, B.; and Cui, D. 2024. Ada-MSHyper: Adaptive Multi-Scale Hypergraph Transformer for Time Series Forecasting. In *Advances in Neural Information Processing Systems*.
- Sherstinsky, A. 2018. Fundamentals of Recurrent Neural Network (RNN) and Long Short-Term Memory (LSTM) Network. *CoRR*, abs/1808.03314.
- Shi, X.; Wang, S.; Nie, Y.; Li, D.; Ye, Z.; Wen, Q.; and Jin, M. 2025. Time-MoE: Billion-Scale Time Series Foundation Models with Mixture of Experts. In *International Conference on Learning Representations*.
- Touvron, H.; Lavril, T.; Izacard, G.; Martinet, X.; Lachaux, M.; Lacroix, T.; Rozière, B.; Goyal, N.; Hambro, E.; Azhar, F.; Rodriguez, A.; Joulin, A.; Grave, E.; and Lample, G. 2023. LLaMA: Open and Efficient Foundation Language Models. *CoRR*, abs/2302.13971.
- Wang, S.; Li, J.; Shi, X.; Ye, Z.; Mo, B.; Lin, W.; Ju, S.; Chu, Z.; and Jin, M. 2025. TimeMixer++: A General Time Series Pattern Machine for Universal Predictive Analysis. In *International Conference on Learning Representations*.
- Wang, Y.; Wu, H.; Dong, J.; Qin, G.; Zhang, H.; Liu, Y.; Qiu, Y.; Wang, J.; and Long, M. 2024. TimeXer: Empowering Transformers for Time Series Forecasting with Exogenous Variables. In *Advances in Neural Information Processing Systems*.
- Wu, H.; Hu, T.; Liu, Y.; Zhou, H.; Wang, J.; and Long, M. 2023. TimesNet: Temporal 2D-Variation Modeling for General Time Series Analysis. In *International Conference on Learning Representations*.
- Xue, H.; and Salim, F. D. 2023. Promptcast: A new prompt-based learning paradigm for time series forecasting. *IEEE Transactions on Knowledge and Data Engineering*, 36(11): 6851–6864.
- Yang, A.; Zhang, B.; Hui, B.; Gao, B.; Yu, B.; Li, C.; Liu, D.; Tu, J.; Zhou, J.; Lin, J.; Lu, K.; Xue, M.; Lin, R.; Liu, T.; Ren, X.; and Zhang, Z. 2024a. Qwen2.5-Math Technical Report: Toward Mathematical Expert Model via Self-Improvement. *CoRR*, abs/2409.12122.
- Yang, R.; Cao, L.; Yang, J.; and *et al.* 2024b. Rethinking Fourier Transform from A Basis Functions Perspective for Long-term Time Series Forecasting. In *Advances in Neural Information Processing Systems*.
- Yeo, K.; Melnyk, I.; Nguyen, N.; and Lee, E. K. 2018. DE-RNN: Forecasting the Probability Density Function of Non-linear Time Series. In *International Conference on Data Mining*, 697–706.
- Zeng, A.; Chen, M.; Zhang, L.; and Xu, Q. 2023. Are Transformers Effective for Time Series Forecasting? In *AAAI Conference on Artificial Intelligence*, 11121–11128.
- Zhang, J.; Zhu, W.; and Gao, J. 2025. Adapting Large Language Models for Time Series Modeling via a Novel Parameter-efficient Adaptation Method. *CoRR*, abs/2502.13725.
- Zhang, L.; Zhang, L.; Shi, S.; Chu, X.; and Li, B. 2023. LoRA-FA: Memory-efficient Low-rank Adaptation for Large Language Models Fine-tuning. *CoRR*, abs/2308.03303.
- Zhang, S.; Roller, S.; Goyal, N.; Artetxe, M.; Chen, M.; Chen, S.; Dewan, C.; Diab, M. T.; Li, X.; Lin, X. V.; Mihaylov, T.; Ott, M.; Shleifer, S.; Shuster, K.; Simig, D.; Koura, P. S.; Sridhar, A.; Wang, T.; and Zettlemoyer, L. 2022. OPT: Open Pre-trained Transformer Language Models. *CoRR*, abs/2205.01068.
- Zhang, Y.; and Yan, J. 2023. Crossformer: Transformer Utilizing Cross-Dimension Dependency for Multivariate Time Series Forecasting. In *International Conference on Learning Representations*.
- Zhong, S.; Ruan, W.; Jin, M.; Li, H.; Wen, Q.; and Liang, Y. 2025. Time-VLM: Exploring Multimodal Vision-Language Models for Augmented Time Series Forecasting. In *International Conference on Machine Learning*.
- Zhou, H.; Zhang, S.; Peng, J.; Zhang, S.; Li, J.; Xiong, H.; and Zhang, W. 2021. Informer: Beyond Efficient Transformer for Long Sequence Time-Series Forecasting. In *AAAI Conference on Artificial Intelligence*, 11106–11115.
- Zhou, T.; Niu, P.; Wang, X.; Sun, L.; and Jin, R. 2023. One Fits All: Power General Time Series Analysis by Pretrained LM. In *Advances in Neural Information Processing Systems*.

Appendix of SE-LLM

Implementation Details of the TSCC Pipeline

The pipeline consists of several interdependent components such as cross-attention, AM-VAE, top-k correlation filtering, and gating fusion. Below, we provide detailed pseudocode for each component to improve readability and explain their roles within the pipeline.

Cross-Modality Alignment. The first step is to align the temporal embeddings with the semantic space using a cross-attention mechanism, where semantic queries attend to temporal keys and values.

Algorithm 2: Cross-Modality Alignment

- 1: **Input:** Temporal sequence `time_seq`, Semantic embeddings `word`.
 - 2: **Output:** Aligned temporal features `aligned_time`.
 - 3: Compute query, key, and value matrices: {Project semantic tokens as queries; temporal tokens as keys/values.}
 - 4: $\mathbf{Q} \leftarrow \text{Query}(\text{word})$
 - 5: $\mathbf{K} \leftarrow \text{Key}(\text{time_seq})$
 - 6: $\mathbf{V} \leftarrow \text{Value}(\text{time_seq})$
 - 7: Calculate attention scores: {Measure similarity between semantic queries and temporal keys.}
 - 8: $\text{attn_scores} \leftarrow \frac{\mathbf{Q} \cdot \mathbf{K}^T}{\sqrt{d_{\text{model}}}}$
 - 9: Apply softmax to get attention weights: {Convert raw scores to normalized attention distribution.}
 - 10: $\text{attn_weights} \leftarrow \text{softmax}(\text{attn_scores})$
 - 11: Compute aligned temporal features: {Weighted aggregation of temporal values guided by semantic queries.}
 - 12: $\text{aligned_time} \leftarrow \text{attn_weights} \cdot \mathbf{V}$
-

Anomaly Pattern Modeling. The AM-VAE module models latent anomaly patterns by estimating the underlying distribution and disentangling anomaly versus non-anomaly semantics.

Temporal Pattern Infusion. We inject temporal correlations into semantics via cross-correlation analysis and top-k filtering.

Algorithm 4: Temporal Pattern Infuse via Top-k Filtering

- 1: **Input:** Temporal feature `DA`, De-anomalized feature `DC`, Cross-correlation matrix `M`.
 - 2: **Output:** Enhanced temporal and semantic features.
 - 3: Compute cross-correlation matrix: {Normalize and correlate temporal vs. semantic representations.}
 - 4: $\mathbf{M} \leftarrow \frac{H - \mu_H}{\sigma_H} \cdot \frac{S^T - \mu_S}{\sigma_S}$
 - 5: Apply top-k filtering: {Select only the strongest temporal-semantic correlations.}
 - 6: $\overline{\mathbf{DA}} \leftarrow \mathbf{DA} \cdot \frac{1}{n} \sum_{i=1}^n \mathcal{P}(S_i, m_{\text{top-k}}^i)$
 - 7: $\overline{\mathbf{DC}} \leftarrow \mathbf{DC} \cdot \frac{1}{n} \sum_{i=1}^n \mathcal{P}(S_i, m_{\text{top-k}}^i)$
-

Gated Fusion. A gate adaptively selects how much temporal vs. semantic information contributes to the fused representation.

Algorithm 3: Anomaly Pattern Modeling via AM-VAE

- 1: **Input:** Cross-attention output `C` (joint space).
 - 2: **Output:** Decomposed anomaly semantic `DC` and de-anomalized semantic `DA`.
 - 3: Project the input to latent space: {Encode joint space representation into latent variables.}
 - 4: $\mathbf{V} \leftarrow \text{Encoder}(\mathbf{C})$
 - 5: Estimate latent distribution: {Predict mean and variance for variational inference.}
 - 6: $\mu, \log \sigma^2 \leftarrow \text{Latent_Distribution}(\mathbf{V})$
 - 7: Apply reparameterization trick: {Sampling latent code with differentiability.}
 - 8: $\mathbf{z} \leftarrow \mu + \epsilon \cdot \exp(0.5 \log \sigma^2)$
 - 9: where $\epsilon \sim \mathcal{N}(0, I)$ is random noise.
 - 10: Decode latent variable: {Generate anomaly semantics from latent representation.}
 - 11: $\mathbf{DC} \leftarrow \text{Decoder}(\mathbf{z})$
 - 12: Compute de-anomaly semantic: {Subtract anomaly component from original to obtain clean semantics.}
 - 13: $\mathbf{DA} = \mathbf{C} - \mathbf{DC}$
-

Algorithm 5: Gated Fusion of Temporal and Semantic Features

- 1: **Input:** Temporal feature `time_feat`, Text feature `text_feat`, Semantic embeddings `word`.
 - 2: **Output:** Fused feature `fused`.
 - 3: Compute similarity: {Match temporal features with the most relevant semantic tokens.}
 - 4: $\text{sim_matrix} \leftarrow \text{matmul}(\text{time_feat}, \text{word}^T)$
 - 5: Select top-k semantic tokens: {Keep only the most relevant semantic dimensions.}
 - 6: $\text{topk_idx} \leftarrow \text{topk}(\text{sim_matrix}, k = 32)$
 - 7: Enhance selected semantic features: {Aggregate top-k semantic cues.}
 - 8: $\text{enhanced_text} \leftarrow \text{mean}(\text{selected_text}, \text{dim} = 1)$
 - 9: Improve semantic alignment: {Normalize and amplify discriminative semantics.}
 - 10: $\text{enhanced_text} \leftarrow \text{softmax}(\text{enhanced_text}, \text{dim} = 1)$
 - 11: Concatenate features: {Prepare inputs for gating network.}
 - 12: $\text{combined} \leftarrow \text{concat}(\text{time_feat}, \text{enhanced_text})$
 - 13: Compute gate values: {Predict adaptive weight between temporal and semantic paths.}
 - 14: $\text{gate} \leftarrow \text{Gate_Net}(\text{combined})$
 - 15: Fuse features: {Final adaptive fusion.}
 - 16: $\text{fused} \leftarrow \text{gate} \cdot \text{time_feat} + (1 - \text{gate}) \cdot \text{text_feat}$
-

Final Model Fusion. Combine anomaly and de-anomaly branches to produce the final enhanced representation. The final fused output is passed through a linear layer or subsequent predictor for forecasting.

Algorithm 6: Final Fusion of Anomaly and De-Anomaly Features

- 1: **Input:** Fused anomaly output, Fused de-anomaly output.
 - 2: **Output:** Final fused output `fused_output`.
 - 3: Combine both outputs: {Residual fusion capturing full semantic spectrum.}
 - 4: `fused_output` \leftarrow `fused_output_da` + `fused_output_dc`
-

Autoregressive Forecasting

In time series forecasting, autoregressive models offer the advantage of making predictions over arbitrary time horizons while being trained solely on sequences of fixed length, thereby significantly reducing computational overhead. These models generate future values by iteratively conditioning on previously observed data points. This strictly sequential inference mechanism leverages the temporal continuity and intrinsic patterns present in historical observations. When these underlying patterns remain stable over time, autoregressive models typically produce reliable and consistent forecasts.

Algorithm 7: Autoregressive Inference with Token Stride τ

Require: Input $\mathbf{X} \in \mathbb{R}^{B \times L \times C}$, stride τ , horizon T .

Ensure: Output $\hat{\mathbf{Y}} \in \mathbb{R}^{B \times T \times C}$.

- 1: $N \leftarrow \lfloor T/\tau \rfloor$
 - 2: $dis \leftarrow T - N \cdot \tau$
 - 3: $K \leftarrow N + \mathbb{I}[dis \neq 0] \{K = \lceil T/\tau \rceil\}$
 - 4: $\mathcal{P} \leftarrow []$ {store predicted chunks}
 - 5: **for** $j \leftarrow 1$ **to** K **do**
 - 6: **if** $j > 1$ **then**
 - 7: $\mathbf{X} \leftarrow \text{Cat}(\mathbf{X}_{:, \tau+1:L, :}, \mathcal{P}_{j-1})$
 - 8: **end if**
 - 9: $\mathbf{O} \leftarrow \text{Model}(\mathbf{X})$
 - 10: $\mathbf{p} \leftarrow \mathbf{O}_{:, end-\tau+1:end, :}$ {last τ steps}
 - 11: append \mathbf{p} to \mathcal{P}
 - 12: **end for**
 - 13: $\hat{\mathbf{Y}} \leftarrow \text{Cat}(\mathcal{P}) \{B \times (K \cdot \tau) \times C\}$
 - 14: **if** $dis \neq 0$ **then**
 - 15: $\hat{\mathbf{Y}} \leftarrow \hat{\mathbf{Y}}_{:, 1:T, :}$ {truncate to T }
 - 16: **end if**
 - 17: **return** $\hat{\mathbf{Y}}$
-

SE-LLM adopts an autoregressive inference strategy, inspired by the design of AutoTimes. Specifically, future values are generated by recursively feeding the model’s prior outputs back into the input sequence as context for subsequent predictions. This iterative process enables long-horizon forecasting while maintaining coherence with the temporal dynamics of the series. The complete inference procedure is summarized in Algorithm 7.

Experiment

Experimental Setup

Evaluation Metrics. Time series forecasting, quantitative evaluation is essential for assessing model performance. In this study, we adopt standard metrics tailored to different forecasting scenarios. For long-term forecasting, we use Mean Squared Error (MSE) and Mean Absolute Error (MAE):

$$\text{MAE} = \frac{1}{N} \sum_{n=1}^N |Y_n - \hat{Y}_n|, \quad (9)$$

$$\text{MSE} = \frac{1}{N} \sum_{n=1}^N (Y_n - \hat{Y}_n)^2. \quad (10)$$

MAE reflects the average magnitude of forecast errors, while MSE penalizes larger deviations more heavily due to the squaring operation. For short-term and zero-shot forecasting on the M4 and M3 dataset, we additionally employ the following metrics:

Mean Absolute Percentage Error (MAPE):

$$\text{MAPE} = \frac{100}{N} \sum_{n=1}^N \frac{|Y_n - \hat{Y}_n|}{|Y_n|}, \quad (11)$$

Symmetric Mean Absolute Percentage Error (SMAPE):

$$\text{SMAPE} = \frac{200}{N} \sum_{n=1}^N \frac{|Y_n - \hat{Y}_n|}{|Y_n| + |\hat{Y}_n|}, \quad (12)$$

Mean Absolute Scaled Error (MASE):

$$\text{MASE} = \frac{1}{N} \sum_{n=1}^N \frac{|Y_n - \hat{Y}_n|}{\frac{1}{N-m} \sum_{j=m+1}^N |Y_j - Y_{j-m}|}, \quad (13)$$

Overall Weighted Average (OWA):

$$\text{OWA} = \frac{1}{2} \left(\frac{\text{SMAPE}}{\text{SMAPE}_{\text{Naive2}}} + \frac{\text{MASE}}{\text{MASE}_{\text{Naive2}}} \right). \quad (14)$$

MAPE and SMAPE provide scale-invariant percentage-based error assessments, with SMAPE mitigating issues related to small denominators. MASE offers a relative comparison against a naive seasonal benchmark. OWA combines MASE and SMAPE relative to the Naive2 baseline, serving as a composite indicator of overall performance.

Datasets. We adopted publicly available benchmarks in four research domains: long-term forecasting, short-term forecasting, zero-shot forecasting and in-context forecasting (Liu et al. 2024c). The experimental datasets comprised: ETTh (Zhou et al. 2021), ETTm (Zhou et al. 2021), Weather (Chen et al. 2021), Elcetricity (ECL) (Chen et al. 2021), Traffic (Chen et al. 2021), Solar (Lai et al. 2018), M3 (Wu et al. 2023), and M4 (Makridakis, Spiliotis, and Assimakopoulos 2020) datasets. The detailed introduction refers to the Table 8. Time series datasets consist of sequential data points collected or recorded at consistent time intervals (e.g., hourly, daily, monthly). Each entry includes a timestamp and one or more observed values. These datasets are used to train models that identify historical patterns to

Table 8: The dataset includes detailed descriptions, with specifications such as dimensionality, the distribution of total time points across training, validation, and test partitions, the target range of future time points for prediction, and the temporal sampling rate.

Tasks	Datasets	Dim	Forecast Horizon	Dataset Size	Frequency	Information
Long-Term Forecasting	ETTh1	7	{96, 192, 336, 720}	{8545, 2881, 2881}	Hourly	Electricity
	Weather	21	{96, 192, 336, 720}	{36792, 5271, 10540}	10min	Weather
	Traffic	862	{96, 192, 336, 720}	{12185, 1757, 3509}	Hourly	Transportation
	ECL	321	{96, 192, 336, 720}	{18317, 2633, 5261}	Hourly	Electricity
	Solar	137	{96, 192, 336, 720}	{36601, 5161, 10417}	10min	Energy
Short-Term Forecasting and Zero-Shot Forecasting	M4-Yearly	1	6	{23000, 0, 23000}	Yearly	Univariate
	M4-Quarterly	1	8	{24000, 0, 24000}	Quarterly	Univariate
	M4-Monthly	1	18	{48000, 0, 48000}	Monthly	Univariate
	M4-Weekly	1	13	{359, 0, 359}	Weekly	Univariate
	M4-Daily	1	14	{4227, 0, 4227}	Daily	Univariate
	M4-Hourly	1	48	{414, 0, 414}	Hourly	Univariate
Zero-Shot Forecasting	M3-Yearly	1	6	{645, 0, 645}	Yearly	Univariate
	M3-Quarterly	1	8	{756, 0, 756}	Quarterly	Univariate
	M3-Monthly	1	18	{1428, 0, 1428}	Monthly	Univariate
	M3-Others	1	8	{174, 0, 174}	Others	Univariate

Table 9: The input length of the SE-LLM is 672. The forecast horizon is {96, 192, 336, 720}. The best results are in red and the second best are blue.

Models		SE-LLM		TimeXier++ 2025		TimeMOE 2025		TQNet 2025		Time-CMA 2025		LLM-TS 2025		AutoTimes-GPT2 2024		Time-LLM 2024		iTransformer 2024	
Datasets	Metrics	MSE	MAE	MSE	MAE	MSE	MAE	MSE	MAE	MSE	MAE	MSE	MAE	MSE	MAE	MSE	MAE	MSE	MAE
ETTh1	96	0.352	0.393	0.375	0.404	0.349	0.379	0.379	0.403	0.366	0.396	0.403	0.420	0.360	0.397	0.398	0.410	0.387	0.418
	192	0.378	0.411	0.415	0.436	0.395	0.413	0.417	0.430	0.401	0.420	0.440	0.441	0.391	0.419	0.451	0.440	0.416	0.437
	336	0.391	0.420	0.442	0.451	0.447	0.453	0.452	0.457	0.412	0.431	0.471	0.457	0.408	0.432	0.473	0.451	0.434	0.450
	720	0.402	0.437	0.482	0.482	0.457	0.462	0.505	0.510	0.406	0.427	0.503	0.487	0.429	0.452	0.469	0.470	0.447	0.473
	avg	0.381	0.415	0.429	0.443	0.412	0.426	0.438	0.450	0.396	0.419	0.454	0.451	0.397	0.425	0.448	0.443	0.421	0.445
Weather	96	0.150	0.200	0.150	0.202	0.198	0.288	0.149	0.202	0.167	0.211	0.166	0.217	0.158	0.208	0.149	0.200	0.174	0.225
	192	0.194	0.243	0.196	0.244	0.235	0.312	0.201	0.249	0.212	0.253	0.229	0.269	0.207	0.264	0.195	0.243	0.227	0.268
	336	0.247	0.285	0.248	0.285	0.293	0.348	0.247	0.287	0.270	0.2927	0.278	0.302	0.262	0.298	0.245	0.282	0.290	0.309
	720	0.323	0.339	0.316	0.332	0.427	0.428	0.312	0.332	0.350	0.348	0.354	0.351	0.342	0.353	0.318	0.338	0.374	0.360
	avg	0.229	0.267	0.228	0.266	0.288	0.344	0.227	0.268	0.250	0.276	0.257	0.285	0.242	0.281	0.227	0.266	0.266	0.291
Traffic	96	0.350	0.243	0.367	0.266	—	—	0.366	0.255	—	—	0.587	0.315	0.369	0.257	0.373	0.280	0.363	0.259
	192	0.373	0.254	0.379	0.364	—	—	0.392	0.276	—	—	0.612	0.326	0.394	0.268	0.390	0.288	0.383	0.267
	336	0.390	0.263	0.417	0.301	—	—	0.400	0.280	—	—	0.634	0.338	0.413	0.278	0.407	0.299	0.396	0.275
	720	0.429	0.285	0.453	0.314	—	—	0.442	0.300	—	—	0.640	0.351	0.449	0.299	0.438	0.310	0.435	0.296
	avg	0.386	0.261	0.404	0.311	—	—	0.400	0.278	—	—	0.618	0.333	0.406	0.276	0.402	0.294	0.394	0.274
ECL	96	0.130	0.225	0.132	0.226	0.157	0.211	0.131	0.228	0.151	0.260	0.167	0.271	0.140	0.236	0.137	0.244	0.133	0.229
	192	0.148	0.242	0.151	0.244	0.208	0.256	0.153	0.251	0.171	0.273	0.178	0.280	0.159	0.253	0.162	0.271	0.151	0.245
	336	0.164	0.259	0.169	0.265	0.255	0.290	0.169	0.268	0.190	0.291	0.198	0.302	0.177	0.270	0.175	0.279	0.168	0.262
	720	0.203	0.293	0.201	0.291	0.405	0.397	0.192	0.287	0.226	0.324	0.233	0.344	0.216	0.303	0.207	0.306	0.205	0.294
	avg	0.161	0.255	0.163	0.257	0.256	0.289	0.161	0.259	0.185	0.287	0.173	0.266	0.173	0.268	0.170	0.275	0.164	0.258
Solar	96	0.165	0.220	0.177	0.235	—	—	0.197	0.244	0.202	0.222	—	—	0.179	0.220	0.224	0.289	0.183	0.265
	192	0.183	0.235	0.190	0.249	—	—	0.230	0.274	0.216	0.240	—	—	0.198	0.236	0.244	0.288	0.205	0.283
	336	0.199	0.248	0.199	0.262	—	—	0.244	0.281	0.236	0.255	—	—	0.213	0.252	0.225	0.291	0.224	0.299
	720	0.219	0.266	0.209	0.276	—	—	0.247	0.280	0.252	0.264	—	—	0.239	0.277	0.243	0.301	0.239	0.316
	avg	0.192	0.242	0.194	0.256	—	—	0.230	0.270	0.227	0.276	—	—	0.207	0.246	0.234	0.293	0.213	0.291

forecast future values. Common applications include predicting stock prices, energy demand, weather, sales, and website traffic.

Baseline. The experiments were conducted and compared with SOTA methods, such as: TimeMixer++ (Wang et al. 2025) and AutoTimes (Liu et al. 2024c) as the high-performance baselines for evaluation. The algorithms involved in all the experiments are TimeMOE (Shi et al. 2025), Time-CMA (Liu et al. 2025), TQNet (Lin et al. 2025), Time-LLM (Jin et al. 2024), LLM-TS (Chen et al. 2025), iTransformer (Liu et al. 2024b), DLinear (Zeng et al. 2023), Time-VLM (Zhong et al. 2025), S2IP-LLM (Pan et al. 2024a), PatchTST (Nie et al. 2023), TimesNet (Wu et al. 2023), FEDFormer (Yang et al. 2024b), Informer (Zhou et al. 2021), Reformer (Kitaev, Kaiser, and Levskaya 2020),

Koopa (Liu et al. 2023), and FPT (Zhou et al. 2023), some of which serve as supplementary references.

Comparative Results

Long Term Forecasting. The full results for long-term series forecasting are shown in Table 9. On the ETTh1, weather, Traffic and Solar datasets, we achieve the best performance. On the Weather datasets, we rank second MAE to TimeMixer++ and Time-LLM. Overall, our performance surpasses current SOTA methods.

Short Term Forecasting. The full results for short-term series forecasting are shown in Table 10. The experimental results indicate that We achieved the best performance in Yearly and Monthly patterns. In the Others pattern, TimeMixer++ achieved the lowest SMAPE, while AutoTimes

Table 10: The M4 dataset includes yearly, quarterly, monthly, weekly, daily, and hourly data, the short-term forecasts averaged across all M4 subsets.

Models		SE-LLM	TimeMixer++ 2025	FSCA 2025	Time-VLM 2025	AutoTimes 2024	S2IP-LLM 2024	Time-LLM 2024	FPT 2024	iTransformer 2024
Yearly	SMAPE	13.294	13.397	13.288	13.419	13.319	13.413	13.419	15.531	13.652
	MASE	2.970	2.990	2.974	3.005	3.021	3.024	3.005	3.015	3.095
	OWA	0.780	0.786	0.781	0.789	0.789	0.792	0.789	0.793	0.807
Quarterly	SMAPE	10.079	10.206	10.037	10.110	10.020	10.352	10.110	10.177	10.353
	MASE	1.177	1.201	1.174	1.178	1.162	1.228	1.178	1.194	1.209
	OWA	0.887	0.901	0.884	0.889	0.878	0.922	0.889	0.897	0.911
Monthly	SMAPE	12.618	12.720	12.762	12.980	12.696	12.995	12.980	12.894	13.079
	MASE	0.931	0.943	0.947	0.963	0.936	0.970	0.963	0.956	0.974
	OWA	0.875	0.884	0.897	0.903	0.880	0.910	0.903	0.897	0.911
Others	SMAPE	4.896	4.593	4.761	4.795	4.916	4.805	4.795	4.940	4.780
	MASE	3.306	3.380	3.207	3.178	3.310	3.247	3.178	3.228	3.231
	OWA	1.037	1.054	1.007	1.006	1.039	1.017	1.006	1.029	1.012
Average	SMAPE	11.778	11.884	11.828	11.894	11.831	12.021	11.983	11.991	12.142
	MASE	1.578	1.597	1.580	1.592	1.585	1.612	1.595	1.600	1.631
	OWA	0.847	0.856	0.850	0.855	0.850	0.857	0.859	0.861	0.874

Table 11: The experimental results are based on the generalization of consistent temporal patterns. For non-matching patterns, we evaluate frequency transfers from Monthly to Weekly/Daily/Hourly in the M3 → M4 dataset, and from Quarterly to other frequencies in the M4 → M3 dataset.

Method		SE-LLM	AutoTimes	FPT	Dlinear	PatchTST	TimesNet	FEDformer	Informer	Reformer
M3→M4	Yearly	13.706	13.708	13.740	14.193	13.966	15.655	13.887	18.542	15.662
	Quarterly	10.718	10.742	10.787	18.856	10.929	11.877	11.513	16.907	11.051
	Monthly	14.553	14.558	14.630	14.765	14.664	16.165	18.154	23.454	15.604
	Others	6.269	6.259	7.081	9.194	7.087	6.863	7.529	7.348	7.001
	Avg	13.024	13.036	13.125	15.337	13.228	14.553	15.047	19.047	14.092
M4→M3	Yearly	13.692	15.731	16.420	17.430	15.990	18.750	16.000	19.700	16.030
	Quarterly	9.011	9.350	10.130	9.740	9.620	12.260	9.480	13.000	9.760
	Monthly	13.978	14.060	14.100	15.650	14.710	14.010	15.120	15.910	14.800
	Others	4.872	5.790	4.810	6.810	9.440	6.880	8.940	13.030	7.530
	Avg	12.560	12.750	13.060	14.030	13.390	14.170	13.530	15.820	13.370

reached the lowest error in Quarterly pattern. From the lowest average error overall, SE-LLM achieve a lower SMAPE, signifying the best forecasting performance.

Zero-Shot Forecasting. The full results for zero-shot forecasting are shown in Table 11. We adopt the zero-shot forecasting methodology from AutoTimes, where each experimental setup involves training a model on a designated source dataset and subsequently deploying it to generate forecasts on a target dataset. These zero-shot scenarios are executed across subsets categorized by their sampling frequencies, each exhibiting distinct distributional properties. Overall, SE-LLM achieves the best performance.

Ablation Study

Ablation on Long-Term Forecasting. The full results of the innovation methods are shown in Table 12. SE-LLM uses cross-domain attention alignment (Jin et al. 2024; Chang et al. 2025; Liu et al. 2025) as the baseline. After replacing it with TSCC, errors were reduced across different LLMs. To make LLMs more suitable for processing time-series data, we incorporated a Time-Adapter, which further improved the model’s predictive performance. The ablation results demonstrate the effectiveness of our innovations.

Ablation on Short-Term Forecasting. The ablation experiments for short-term forecasting are presented in the Table 13. We compared the performance by replacing different Large Language Models (LLMs) with SE-LLM on the M4 dataset. The findings indicate that LLama exhibits lower errors, followed by Qwen2.5-0.5B.

Ablation on Adapters. We use the best-performing Qwen2.5-0.5B model as the baseline and evaluate the proposed Time-Adapter’s performance on time-series forecasting tasks. The results are compared to the LoRA adapter. The LoRA parameter configuration is kept consistent with the Time-Adapter, with a rank of 8 and the full ablation results are presented in Table 14. The comparison protocol involves evaluating both adapters across several time-series datasets, specifically focusing on the performance metrics for each dataset. Our findings reveal that the LoRA adapter shows improvements in only the weather and ECL datasets, whereas the Time-Adapter consistently enhances performance across all datasets. In particular, the error reduction is most notable in the weather dataset, where the Time-Adapter achieves a 5.4% decrease in MSE compared to the baseline. This suggests that the Time-Adapter provides a more generalized performance boost across diverse

Table 12: In the ablation experiments, we set the input length to 672 and the output length to 96, with forecast lengths from the set {96, 192, 336, 720}.

LLM		GPT2				Bert				Opt125m				Qwen2.5-0.5B			
Dataset		ECL		Traffic		ECL		Traffic		ECL		Traffic		ECL		Traffic	
Metric		MSE	MAE														
Baseline	96	0.145	0.240	0.387	0.267	0.150	0.245	0.440	0.304	0.140	0.237	0.368	0.258	0.135	0.233	0.373	0.263
	192	0.165	0.257	0.410	0.277	0.168	0.262	0.459	0.314	0.158	0.254	0.390	0.268	0.152	0.249	0.394	0.272
	336	0.183	0.275	0.427	0.286	0.187	0.281	0.476	0.322	0.176	0.272	0.407	0.292	0.170	0.267	0.409	0.280
	720	0.224	0.309	0.463	0.306	0.230	0.316	0.514	0.344	0.216	0.305	0.445	0.300	0.212	0.303	0.444	0.300
	Avg	0.179	0.270	0.422	0.284	0.184	0.276	0.472	0.321	0.173	0.267	0.403	0.280	0.167	0.263	0.405	0.279
+TSCC	96	0.138	0.233	0.368	0.257	0.144	0.240	0.395	0.277	0.136	0.232	0.361	0.251	0.134	0.231	0.356	0.247
	192	0.157	0.250	0.393	0.269	0.161	0.256	0.417	0.286	0.154	0.249	0.383	0.263	0.152	0.248	0.377	0.257
	336	0.176	0.269	0.414	0.281	0.181	0.274	0.436	0.295	0.173	0.267	0.401	0.271	0.169	0.266	0.393	0.266
	720	0.218	0.305	0.461	0.312	0.223	0.309	0.474	0.316	0.215	0.303	0.439	0.294	0.210	0.301	0.431	0.287
	Avg	0.172	0.264	0.409	0.280	0.177	0.270	0.431	0.294	0.170	0.263	0.396	0.270	0.166	0.262	0.389	0.264
+Time-Adapter	96	0.133	0.227	0.363	0.255	0.135	0.230	0.378	0.266	0.132	0.227	0.354	0.247	0.130	0.225	0.350	0.243
	192	0.152	0.244	0.388	0.267	0.152	0.247	0.400	0.275	0.149	0.243	0.378	0.258	0.148	0.242	0.373	0.254
	336	0.169	0.262	0.411	0.281	0.170	0.265	0.417	0.283	0.166	0.261	0.396	0.267	0.164	0.259	0.390	0.263
	720	0.211	0.299	0.461	0.314	0.209	0.298	0.454	0.303	0.204	0.295	0.434	0.291	0.203	0.293	0.429	0.285
	Avg	0.166	0.258	0.406	0.279	0.167	0.260	0.412	0.282	0.163	0.257	0.391	0.266	0.161	0.255	0.386	0.261

Table 13: The first column represents different LLMs replaced based on SE-LLM. "Others" is obtained by averaging the results from the weekly, daily, and hourly periods. The values in **bold** represent the average results, while **red** indicates the best performance, followed by **blue**.

	LLM	GPT2	Bert	Opt-125m	Qwen2.5	Llama
Year	sMAPE	13.843	15.659	14.028	13.396	13.294
	MASE	3.199	3.674	3.198	3.002	2.970
	OWA	0.826	0.941	0.832	0.788	0.780
Quarterly	sMAPE	10.300	12.237	10.320	10.168	10.079
	MASE	1.198	1.573	1.207	1.182	1.177
	OWA	0.904	1.129	0.909	0.893	0.887
Monthly	sMAPE	12.935	14.376	13.273	12.738	12.618
	MASE	0.957	1.118	1.021	0.938	0.931
	OWA	0.898	1.024	0.940	0.883	0.875
Others	sMAPE	5.061	6.358	5.191	4.998	4.896
	MASE	3.468	4.367	3.507	3.417	3.306
	OWA	1.079	1.358	1.099	1.065	1.037
Average	sMAPE	12.121	13.757	12.334	11.886	11.778
	MASE	1.660	1.977	1.691	1.595	1.578
	OWA	0.881	1.024	0.897	0.855	0.847

Table 14: Time-Adapter compared with LoRA. The input length is 672 and forecasting horizons were set to {96, 192, 336, 720}.

Datasets		ETTh1		Weather		Traffic		ECL		Solar	
Metrics		MSE	MAE								
TSCC	96	0.352	0.393	0.162	0.245	0.356	0.247	0.134	0.231	0.175	0.230
	192	0.378	0.411	0.209	0.259	0.377	0.257	0.152	0.248	0.194	0.245
	336	0.391	0.420	0.263	0.299	0.393	0.266	0.169	0.266	0.209	0.257
	720	0.402	0.437	0.332	0.346	0.431	0.287	0.210	0.301	0.227	0.270
	Avg	0.381	0.415	0.242	0.287	0.389	0.264	0.166	0.262	0.201	0.251
+LoRA	96	0.362	0.399	0.157	0.210	0.357	0.251	0.132	0.228	0.173	0.228
	192	0.393	0.420	0.204	0.254	0.378	0.260	0.149	0.244	0.194	0.245
	336	0.410	0.432	0.260	0.297	0.394	0.269	0.166	0.261	0.210	0.260
	720	0.418	0.447	0.339	0.351	0.430	0.290	0.205	0.295	0.229	0.277
	Avg	0.396	0.425	0.240	0.278	0.390	0.268	0.163	0.257	0.202	0.253
+Time-Adapter	96	0.355	0.398	0.150	0.200	0.350	0.243	0.130	0.225	0.165	0.220
	192	0.389	0.421	0.194	0.243	0.373	0.254	0.148	0.242	0.183	0.236
	336	0.409	0.435	0.247	0.285	0.390	0.263	0.164	0.259	0.199	0.249
	720	0.418	0.448	0.323	0.339	0.429	0.285	0.203	0.293	0.219	0.266
	Avg	0.393	0.426	0.229	0.267	0.386	0.261	0.161	0.255	0.192	0.243

time-series data, as compared to LoRA.

Ablation on LLM-based SOTA methods. In this paper, we propose TSCC and Time-Adapter to enhance the interpretability of LLMs. Furthermore, we integrate our methods into Time-LLM, AutoTimes, and Time-CMA. However, due to inherent algorithmic constraints, Time-CMA relies solely on the LLM to extract textual descriptions of time-series data and thus cannot incorporate Time-Adapter. In Table 15, we present the performance enhancement achieved by our method in long-term forecasting compared to current research. It is worth noting that the original autoregressive forecasting paradigm of AutoTimes is not well suited for the ETT dataset. Therefore, we make several modifications in our implementation. Specifically, the LLM component is instantiated with GPT-2, a multi-step forecasting strategy is adopted instead of autoregressive prediction, and temporal positional encodings are integrated at the input level.

Statistical Stability. To ensure the reliability and reproducibility of our results, all experiments are conducted under random seeds corresponding to 2024, 2025, and 2026. For each forecasting horizon, we report the mean and standard deviation of MSE and MAE across repeated runs under these seeds. This evaluation protocol mitigates randomness arising from parameter initialization, data shuffling, and stochastic optimization dynamics. We note that, due to differences in environment configurations and hardware-dependent behaviors, the LLM-based modules may introduce slight numerical variability, leading to minor fluctuations in prediction performance within a range of approximately ± 0.01 . Such variations are expected and do not affect the overall conclusions. Table 16 reports the forecasting results of SE-LLM under the three random seeds across five datasets and four forecasting horizons. The standard deviations of both MSE and MAE remain consistently small, indicating that the model is largely insensitive to random initialization and environmental perturbations. This stability holds across long-sequence datasets and different forecasting ranges, demonstrating that SE-LLM delivers robust and reproducible performance.

Discussion

The proposed TSCC and Time-Adapter modules are designed to explicitly bridge the gap between large language models and time series forecasting from a modeling perspective. Rather than directly transferring language models to temporal data through prompt engineering or token-level alignment alone, TSCC focuses on enriching semantic representations with structured temporal correlations, while the Time-Adapter addresses the mismatch in temporal dependency modeling by explicitly capturing both long-term and short-term dynamics. Experimental results demonstrate that the general knowledge encoded in pre-trained language models is insufficient for structured temporal reasoning unless it is coupled with mechanisms that explicitly encode temporal structure, dependencies, and variability. From this perspective, our work suggests a principled direction for future research on aligning foundation models with structured non-linguistic data, where adaptation should be guided by

the intrinsic properties of the target domain rather than relying on superficial modality conversion.

Limitation

We provide further clarification on the limitations of SE-LLM. Firstly, in short-term and zero-shot forecasting using the LLama model, Time-Adapter was not employed in all instances due to computational constraints, which contradicts the low computational cost objective of this paper. As a result, Time-Adapter was excluded from these experiments. In fact, incorporating Time-Adapter in specific layers would likely lead to performance improvements. However, due to concerns about computational costs, we did not pursue this avenue in the current study. Additionally, LLama was not considered for long-term forecasting due to its generally poor performance and high computational demands.

The Use of LLMs

This paper employs a large language model (LLM) to check for spelling errors, correct grammar, and refine the language.

Table 15: The results were conducted in the ETTh1, ETTh2, ETTm1, and ETTm2 datasets. The **Baseline** represents our reproduced results, which differ from those in the original paper. Under the same parameters, we added TSCC and Time-Adapter. The forecasting horizons were set to {96, 192, 336, 720}.

Methods		Time-LLM		TSCC		Time-Adapter		AutoTimes		TSCC		Time-Adapter		Time-CMA		TSCC	
Metrics		MSE	MAE														
ETTh1	96	0.384	0.411	0.373	0.401	0.368	0.400	0.360	0.397	0.354	0.394	0.352	0.393	0.393	0.414	0.377	0.396
	192	0.414	0.430	0.403	0.425	0.401	0.421	0.391	0.419	0.385	0.415	0.383	0.414	0.435	0.437	0.429	0.424
	336	0.433	0.448	0.414	0.430	0.412	0.430	0.408	0.432	0.401	0.427	0.399	0.425	0.472	0.453	0.468	0.444
	720	0.448	0.468	0.436	0.460	0.439	0.459	0.429	0.452	0.420	0.446	0.417	0.446	0.482	0.479	0.474	0.471
	Avg	0.420	0.439	0.407	0.429	0.405	0.428	0.397	0.425	0.390	0.421	0.388	0.420	0.446	0.446	0.437	0.434
ETTh2	96	0.293	0.349	0.287	0.352	0.294	0.347	0.288	0.352	0.288	0.352	0.285	0.377	0.339	0.378	0.299	0.347
	192	0.379	0.400	0.367	0.393	0.370	0.400	0.351	0.395	0.350	0.393	0.351	0.390	0.421	0.425	0.377	0.395
	336	0.381	0.414	0.390	0.414	0.373	0.402	0.383	0.424	0.378	0.419	0.376	0.413	0.452	0.452	0.415	0.426
	720	0.428	0.452	0.426	0.446	0.418	0.445	0.447	0.468	0.435	0.461	0.416	0.446	0.452	0.462	0.424	0.443
	Avg	0.370	0.404	0.368	0.401	0.364	0.399	0.367	0.410	0.363	0.406	0.357	0.407	0.416	0.429	0.379	0.403
ETTh1	96	0.300	0.356	0.302	0.354	0.303	0.354	0.291	0.347	0.286	0.341	0.285	0.340	0.340	0.380	0.311	0.352
	192	0.340	0.378	0.341	0.378	0.345	0.376	0.338	0.376	0.334	0.371	0.332	0.369	0.379	0.407	0.360	0.381
	336	0.370	0.395	0.373	0.399	0.366	0.394	0.376	0.398	0.370	0.394	0.366	0.392	0.405	0.413	0.396	0.405
	720	0.422	0.428	0.422	0.427	0.414	0.428	0.438	0.433	0.427	0.429	0.421	0.426	0.472	0.450	0.464	0.444
	Avg	0.358	0.389	0.360	0.390	0.357	0.388	0.361	0.389	0.354	0.384	0.351	0.382	0.399	0.413	0.383	0.396
ETTh2	96	0.172	0.265	0.180	0.270	0.178	0.268	0.176	0.264	0.174	0.261	0.173	0.262	0.191	0.274	0.173	0.256
	192	0.232	0.306	0.247	0.314	0.229	0.303	0.238	0.307	0.236	0.303	0.234	0.302	0.257	0.316	0.242	0.301
	336	0.281	0.339	0.276	0.335	0.291	0.342	0.298	0.346	0.291	0.341	0.291	0.337	0.313	0.350	0.307	0.323
	720	0.362	0.387	0.366	0.391	0.364	0.391	0.382	0.400	0.373	0.394	0.373	0.389	0.416	0.407	0.416	0.407
	Avg	0.262	0.324	0.267	0.328	0.266	0.326	0.274	0.329	0.269	0.325	0.268	0.323	0.294	0.337	0.285	0.322

Table 16: Performance stability under different random seeds (three runs). For each dataset and forecasting horizon, we report the results from three independent runs (2024, 2025, 2026 seeds), together with the averaged performance (mean) and variability (std). The consistently low standard deviations across all datasets indicate that SE-LLM is robust to randomness in initialization and training, demonstrating stable forecasting performance.

		2024		2025		2026		mean		std	
		MSE	MAE	MSE	MAE	MSE	MAE	MSE	MAE	MSE	MAE
ETTh	96	0.352	0.393	0.355	0.394	0.355	0.394	0.354000	0.393667	0.001414	0.000471
	192	0.378	0.411	0.382	0.412	0.382	0.412	0.380667	0.411667	0.001886	0.000471
	336	0.391	0.420	0.394	0.421	0.394	0.421	0.393000	0.420667	0.001414	0.000471
	720	0.402	0.437	0.405	0.438	0.405	0.439	0.404000	0.438000	0.001414	0.000816
	Avg	0.381	0.415	0.384	0.416	0.384	0.417	0.383000	0.416000	0.001414	0.000816
Weather	96	0.150	0.200	0.152	0.202	0.151	0.202	0.151000	0.201333	0.000816	0.000943
	192	0.194	0.243	0.200	0.249	0.198	0.247	0.197333	0.246333	0.002494	0.002494
	336	0.247	0.285	0.256	0.292	0.253	0.291	0.252000	0.289333	0.003742	0.003091
	720	0.323	0.339	0.328	0.343	0.324	0.337	0.325000	0.339667	0.002160	0.002494
	Avg	0.229	0.267	0.234	0.272	0.232	0.269	0.231667	0.269333	0.002055	0.002055
Traffic	96	0.350	0.243	0.351	0.244	0.351	0.246	0.350667	0.244333	0.000471	0.001247
	192	0.373	0.254	0.373	0.254	0.375	0.256	0.373667	0.254667	0.000943	0.000943
	336	0.390	0.263	0.389	0.263	0.390	0.264	0.389667	0.263333	0.000471	0.000471
	720	0.429	0.285	0.427	0.284	0.428	0.285	0.428000	0.284667	0.000816	0.000471
	Avg	0.386	0.261	0.385	0.261	0.386	0.263	0.385667	0.261667	0.000471	0.000943
ECL	96	0.130	0.225	0.133	0.228	0.134	0.231	0.132333	0.228000	0.001700	0.002449
	192	0.148	0.242	0.151	0.244	0.152	0.247	0.150333	0.244333	0.001700	0.002055
	336	0.164	0.259	0.167	0.262	0.167	0.262	0.166000	0.261000	0.001414	0.001414
	720	0.203	0.293	0.208	0.292	0.208	0.299	0.206333	0.294667	0.002357	0.003091
	Avg	0.161	0.255	0.165	0.257	0.165	0.260	0.163667	0.257333	0.001886	0.002055
Solar	96	0.165	0.220	0.168	0.220	0.167	0.225	0.166667	0.221667	0.001247	0.002357
	192	0.183	0.236	0.188	0.236	0.186	0.241	0.185667	0.237667	0.002055	0.002357
	336	0.199	0.249	0.206	0.251	0.202	0.255	0.202333	0.251667	0.002867	0.002494
	720	0.219	0.266	0.224	0.267	0.220	0.272	0.221000	0.268333	0.002160	0.002625
	Avg	0.192	0.243	0.197	0.244	0.194	0.248	0.194333	0.245000	0.002055	0.002160